

© Copyright 2018

Vega Shah

Shifting role of chemoautotrophic SUP05 bacteria in nitrogen, sulfur and carbon cycles across
oxygen gradients in marine environments

Vega Shah

A dissertation

Submitted in partial fulfillment of the

Requirements for the degree of

Doctor of Philosophy

University of Washington

2018

Reading Committee:

Robert M. Morris, Chair

E. Virginia Armbrust

John A. Baross

Program Authorized to Offer Degree:

School of Oceanography
University of Washington

ABSTRACT

Shifting role of chemoautotrophic SUP05 bacteria in nitrogen, sulfur and carbon cycles across oxygen gradients in marine environments

Vega Shah

Chair of the Supervisory Committee:
Professor Robert M. Morris
School of Oceanography

Microbes make up a large percentage of the biomass within marine environments and play a key role in cycling of biogeochemical cycles. Despite this, majority of important species of bacteria and archaea remain poorly understood due to lack of cultured representatives. Ecological studies have utilized macromolecules like small subunit RNA (16S) to identify and enumerate important groups of microbes in the environment. An uncultivated group of thiotrophic gamma-proteobacteria from the clade SUP05 are ubiquitous and abundant at the interface at the boundaries of marine oxygen minimum zones (OMZs). Metagenomic studies have shown that they play an important role in the cycling of nitrogen, carbon and sulfur within OMZs. In this thesis, I present the first cultivated representative from the chemoautotrophic SUP05 subclade, Candidatus *Thioglobus autotrophicus* along with its complete and annotated genome. SUP05 bacteria have been long suspected as important players in the nitrogen, carbon and sulfur cycles within OMZs. Particularly in processes that involve loss of fixed nitrogen in the form of gases (denitrification) and fixation of carbon. Using laboratory experiments on *T. autotrophicus*, I show

that SUP05 bacteria produce large amounts of nitrite by carrying out dissimilatory nitrate reduction and consuming ammonia. Furthermore, I use growth experiments, cryo-electron tomography and protein expression data *T. autotrophicus* in aerobic and anaerobic to show that SUP05 have the potential to assimilate more carbon and store large amounts of reduced sulfur when they are exposed to oxic environments. This thesis provides a cultured representative of the chemoautotrophic SUP05 and a working model of its growth and metabolic constraints.

TABLE OF CONTENTS

| | |
|---|----|
| List of Figures | 12 |
| List of Tables | 13 |
| Introduction..... | 16 |
| Chapter 1. The genome sequence of <i>Thioglobus autotrophicus</i> strain EF1, a chemoautotroph from the SUP05 clade of marine gamma-proteobacteria | 26 |
| 1.1 Abstract..... | 26 |
| 1.2 Introduction..... | 27 |
| 1.3 Methods..... | 27 |
| 1.4 Results..... | 29 |
| 1.5 References..... | 32 |
| Chapter 2. Cultivation of a chemoautotroph from the SUP05 clade of marine bacteria that produces nitrite and consumes ammonia | 37 |
| 2.1 Abstract | 37 |
| 2.2 Introduction..... | 38 |
| 2.3 Materials and Methods..... | 39 |
| 2.4 Results and Discussion..... | 41 |
| 2.5 Conclusion..... | 47 |
| 2.6 References..... | 49 |
| 2.7 Additional Information..... | 58 |
| 2.8 Supplementary References..... | 60 |
| 2.9 Acknowledgements..... | 66 |

| | |
|--|-----|
| Chapter 3. Oxygen drives dramatic shifts in the metabolic activity of chemoautotrophic SUP05 isolate, Candidatus <i>Thioglobus autotrophicus</i> | 67 |
| 3.1 Abstract..... | 70 |
| 3.2 Introduction..... | 69 |
| 3.3 Materials and Methods..... | 70 |
| 3.4 Results..... | 80 |
| 3.5 Discussion..... | 83 |
| 3.6 References..... | 86 |
| 3.7 Acknowledgements..... | 89 |
| Conclusion..... | 111 |
| Appendix A..... | 113 |
| Curriculum vitae..... | |

LIST OF FIGURES

| | |
|--------------------------------|-----|
| Figure 1.1..... | 35 |
| Figure 2.1..... | 54 |
| Figure 2.2 | 55 |
| Figure 2.3 | 56 |
| Figure 2.4 | 57 |
| Supplementary Figure 2.1 | 62 |
| Supplementary Figure 2.2 | 63 |
| Supplementary Figure 2.3 | 64 |
| Supplementary Figure 2.4 | 65 |
| Figure 3.1 | 92 |
| Figure 3.2 | 93 |
| Figure 3.3 | 95 |
| Figure 3.4 | 96 |
| Figure 3.5 | 97 |
| Supplementary Figure 3.1 | 98 |
| Supplementary Figure 3.2 | 99 |
| Supplementary Figure 3.3 | 100 |
| Supplementary Figure 3.4 | 101 |
| Supplementary Figure 3.5 | 102 |

LIST OF TABLES

| | |
|-------------------------------|-----|
| Table 1.1..... | 36 |
| Supplementary Table 2.1 | 61 |
| Supplementary Table 2.2 | 55 |
| Table 3.1..... | 90 |
| Table 3.2 | 91 |
| Supplementary Table 3.1 | 103 |
| Supplementary Table 3.2 | 104 |
| Table Appendix A.1 | 110 |

ACKNOWLEDGEMENTS

I would like to thank my advisor Bob for taking a chance on me and accepting me as his second graduate student ever. Over the course of my graduate career, he encouraged me to take chances and explore ideas and experiments while still keeping me focused on the goal of graduating. He also infected me with his optimism and made me see the positive side of people in the science community and for that I am a better person.

I would like to thank my committee members John, Ginger and Deb who have been with me since the beginning and also my GSR, Drew. All the discussions and feedback I received from all of you made my research and writing more impactful.

A heartfelt thank you to my mother, brother and father, Tripti, Vyom and Hemant Shah respectively. You have each supported me in your own special way. Thank you for being there for me when I needed you the most. I hope I can always make you proud.

To all my friends and colleagues in CEG, thank you for being my Seattle science family. The research I produced is relevant because of your hard work and support. To my ‘beastie’ and dear colleague Helena van Tol, we will always be sisters. Your level-headed presence and sharp insight on science and life have kept me grounded. To Tyler Lebrun, Danesh Mondegarian, Melana Yanos and Polina Kud thank you for the hugs, baked pastries, good humor and encouragement. And finally, a big thanks to my friends in the Seattle table tennis community who provided me with endless fun and exercise.

DEDICATION

To Ma and Vyom

INTRODUCTION

Microorganisms although unseen, make up a large volume of the biosphere on planet Earth and play an important role in various key elemental cycles. Bacteria and archaea mediate biogeochemical reactions that maintain the current chemical composition of the atmosphere, terrestrial environments and aquatic environments. Studies have shown that the ocean is one of the largest reservoirs for microorganisms. Estimates indicate that the ocean contains approximately 10^4 to 10^7 cells/ml and taking into account the depth and extent of the ocean, a total of 3.5×10^{30} cells (Whitman et al 1998). Ocean microbes account for approximately 303 Pg of carbon, 85 Pg of nitrogen and 9 Pg of phosphorus (Wiebe et al 1998), all of which are elements essential for life. Although ubiquitous in the marine environment, microbes have been difficult to classify due to their resistance to being cultured in laboratory environments.

Traditional microbiological techniques employ the use of growth media (solid agar or liquid) to culture microbes from environmental samples. But early studies found that these growth methods fell short in accurately representing the abundance and diversity of microbes in the environment, resulting in the phenomena dubbed as 'The Great Plate Count Anomaly' (Staley & Konopka 1985). The great plate count anomaly refers to the difference in diversity and abundance between cells measured directly from the environment versus colony forming microbes grown in lab from the same samples. This effect is especially pronounced in marine environments where only 0.01 to 0.1% of marine bacterial cells produce colonies by standard plating techniques (Giovannoni & Connon 2002).

Molecular techniques have been used as an alternative to culturing bacteria. Microbes can be enumerated and identified by collection and sequencing of nucleotides from the environment

(DNA, RNA). Specific sequences can be targeted and amplified using oligonucleotide probes and methods like polymerase chain reaction (PCR). Most molecular methods in the field of microbial ecology involve use of a single highly conserved region of the bacterial genome, the small subunit of the ribosomal RNA (16S). Collection and sequencing of 16S obtained from the field has been used to identify and quantify different organisms in the ocean. However molecular methods are not sufficient to describe the activity of uncultured microbes. Biogeochemical studies have shown that dominant uncultured microbial groups are responsible for large volume transformations within key elemental cycles within the ocean. But in the absence of cultured representatives and complete genomic sequences, the exact activity of important groups of bacteria and archaea remain a mystery.

Parts of the ocean consist of oxygen depleted, nitrogen rich water that are described as the oxygen minimum zones (OMZs). Due to the lack of oxygen, an important electron acceptor, the primary players in OMZs tend to be microorganisms. OMZs support a wide variety of microbial communities that influence biogeochemical cycles. In particular, microbes at OMZs are responsible for fixed nitrogen loss, heterotrophic and autotrophic carbon metabolism and sulfur metabolism. Oxygen minimum zones form and persist in the ocean when the rate of dissolved oxygen (DO) consumption outcompetes ventilation. OMZs are typically characterized by DO concentrations that range from $<2 \mu\text{mol per kg}$ to as high as $90 \mu\text{mol per kg}$ (Lam and Kuypers 2011, Wright et al 2012). Mid-depth oxygen minimum zones form at nutrient rich upwelling zones where sinking organic matter triggers rapid uptake of oxygen via heterotrophic bacteria. Whereas in coastal regions, OMZs form when seasonal, wind-driven mixing brings nutrient rich water to the surface that contributes to phytoplankton blooms. Heterotrophic microbial

communities resulting in rapid uptake of dissolved organic matter degrade the organic matter produced by primary producers. The effect of this is compounded in fjords with narrow basins and shallow sills that restrict water circulation. Examples of such restricted basins include coastal fjords like Saanich and Effingham inlets in British Columbia (Zaikova et al 2010, Wright et al 2012). OMZs that form in fjords and coastal upwelling regions experience seasonal plumes of hydrogen sulfide produced via the metabolic activity of sulfate reducing bacteria in sediments.

Thiotrophic gamma-proteobacteria belonging to the subclade SUP05 have been found abundant at sulfidic OMZs (Wright et al 2012, Ulloa et al 2012) and also within the cryptic sulfur cycle at a permanent OMZ off the coast of Peru and Chile in the Eastern Tropical South Pacific (ETSP) (Canfield et al 2010). SUP05 bacteria were originally discovered and classified as autotrophic, sulfur oxidizing endosymbionts in the gills of clams, such as *Calyptogena sp.* and *Vesicomya sp.*, in hydrothermal vents and in cold seeps (Dyksma et al 2016). 16S rRNA based diversity analyses in hydrothermal plumes of the Suiyo seamount off the coast of Japan led to the discovery of a highly abundant, free-living gammaproteobacteria closely related to these symbiotic bacteria (Sunamara et al 2004). Until recently, an uncultured lineage, SUP05 bacteria have been primarily studied using a variety of cultivation-independent methods (Walsh et al 2009, Anantharaman et al 2013, Glaubitz et al 2013, Mattes et al 2013, Murillo et al 2014, Hawley et al 2014). These studies suggest that they have critical roles in the nitrogen, sulfur and carbon cycles within OMZs (Walsh et al 2009, Canfield et al 2010).

In the last decade, a variety of new culturing methods have enabled microbial ecologists to successfully cultivate uncultured microbial species and subsequently sequence their whole

genomes. The high throughput cultivation (HTC) method has successfully yielded a number of important isolates and works particularly well in isolating a number of microbes from low nutrient (oligotrophic environments) with typically low cell densities (Connon & Giovannoni 2002). Isolates include individuals from SAR11, OM43, SAR92 and OM60 that are consistently found in environmental clone libraries but had never been cultured before. In chapter 1, I use the high throughput cultivation methods with modifications for low oxygen environments to isolate the first cultivated representative organism from the chemoautotrophic SUP05 clade, from Saanich Inlet (Vancouver Island, BC), a seasonally anoxic coastal fjord. The isolate titled *Candidatus Thioglobus autotrophicus* strain EF1 (Etymology: au.to.tro'phi.cus. Gr. n. autos self; Gr. adj. trophikos nursing, tending or feeding; N.L. masc. adj. autotrophicus autotroph). Additionally, in this chapter I present the closed circular genome of *T.autotrophicus* that further elucidates its genomic potential to mediate chemical transformations involving the nitrogen, sulfur and carbon cycles within low oxygen zones of the ocean.

Oxygen minimum zones play an essential role in the global nitrogen cycle. Studies have shown that approximately half of all fixed nitrogen is lost via microbial metabolism at OMZs (Codispoti et al 2001). In addition, OMZs are also involved in cycling important climactic gases. Specifically, production of approximately 50% of all N₂O (Bange et al 1996) and sequestration of CO₂, via chemosynthetic organisms in the dark ocean (Taylor et al 2001, Schunk et al 2013). Global climate models predict that marine OMZs will not only expand, but also become more persistent in the future (Stramma et al 2008). As OMZs expand, the biogeochemical roles of organisms inhabiting these regions have become increasingly important to study. Nitrogen loss in OMZs has been attributed to two microbially mediated processes, heterotrophic denitrification

and anaerobic ammonium oxidation (anammox) (Francis et al 2007). Heterotrophic denitrification was considered the primary process of nitrogen removal, but recent evidence suggests that anammox accounts for higher N_2 production than heterotrophic denitrification in some OMZs (Lam et al 2009). In the absence of remineralization of organic matter via heterotrophic denitrifiers, the source of ammonium that is essential for anammox associated N_2 production is unclear. SUP05 are suspected to carry out dissimilatory nitrate reduction to ammonium (DNRA), fueling anammox (Wright et al 2012, Hawley et al 2014), and to carry out dissimilatory nitrate reduction, using nitrate (nar and nap), nitrite (nir) and nitrous oxide (nor) genes (Walsh et al 2009, Hawley et al 2014). These studies suggest that SUP05 cells contribute to nitrogen loss in OMZs by producing ammonium required for anammox or by reducing key intermediates in denitrification. In Chapter 2, I use growth experiments to show that *T. autotrophicus* is a facultatively anaerobic sulfur-oxidizing chemolithoautotroph that produces nitrite and is limited for growth via the supply of nitrate and ammonium.

The ocean is a massive reservoir of sulfur, primarily found in the form of sulfate (dissolved) and minerals like pyrite and gypsum. It occurs in a variety of valence states that range from the very reduced (-2) to the very oxidized (+6). Inorganic sulfur can be found in the form of sulfate (most stable form), elemental sulfur, sulfide, thiosulfate and polythionates. Sulfur is an essential element for life and a small fraction (~1%) of it can be found in biomass. This organic sulfur usually exists in the form of S-containing amino acids like cysteine, methionine and taurine. In the surface ocean, phytoplankton can convert methionine to a highly stable and soluble organic compound called DMPS (dimethylsulfoniopropionate). Apart from assimilation, many bacteria and archaea use sulfur in energy producing reactions, also called dissimilatory sulfur

metabolism. Sulfur compounds can act as electron acceptors (sulfate reduction) or electron donors (sulfur oxidation) in these energy-yielding reactions. Both these processes play an important role in oxygen depleted, nitrate-rich marine water.

In “sulfidic” OMZs, reduced sulfur fuels the growth of an array of chemosynthetic bacteria (Zaikova et al 2010, Mattes et al 2013, Ulloa et al 2013). SUP05 bacteria are abundant in fjords that undergo seasonal sulfide enrichment (Walsh et al 2009, Hawley et al 2014, Lavik et al 2009) and in permanently sulfidic OMZs like the Black Sea (Glaubitz et al 2013). SUP05 also thrive in OMZs that are nitrate-rich and sulfide-poor. Canfield and colleagues theorized that there exists a ‘cryptic’ sulfur cycle in these regions, wherein products of sulfate reduction are rapidly oxidized by thiotrophic bacteria (Canfield et al 2010, Teske 2010). Researchers have theorized that organisms within the cryptic sulfur cycle may utilize below detection limit sulfur or alternate sources of reduced sulfur (organic) that were previously not considered viable sources of energy for dissimilatory sulfur cycling (Teske 2010). Current research does not clarify the exact role of SUP05 within the cryptic sulfur cycle; especially it’s nuances at the interface between oxic and anoxic environments. In chapter 3, I test aforementioned hypotheses using growth experiments; electron micrographs and proteomic data obtained from *T.autotrophicus* cells grown in anaerobic versus aerobic environments. I provide evidence that *T.autotrophicus* cells can grow in the presence of below-detection concentrations of reduced sulfur both in a the inorganic and organic form. This experiment being a rare instance of a free living marine microbe using an organic source of sulfur for energy. Cryo-electron images and proteomic data show that *T.autotrophicus* cells display stark differences in physiology, cell structure and constituents in the presence of oxygen. Finally protein data also highlight key proteins that are highly abundant and conserved

(structural proteins) in *T.autotrophicus* that can be used as markers to enumerate and study active SUP05 cells in the environment.

REFERENCES

1. Anantharaman K, Breier JA, Sheik CS, Dick GJ. (2013). Evidence for hydrogen oxidation and metabolic plasticity in widespread deep-sea sulfur-oxidizing bacteria. *Proc Natl Acad Sci U S A* **110**: 330–5.
2. Canfield DE, Stewart FJ, Thamdrup B, De Brabandere L, Dalsgaard T, Delong EF, *et al.* (2010). A cryptic sulfur cycle in oxygen minimum zone waters off the Chilean coast. *Science* (80-) **330**: 1375–1378.
3. Connon SA, Giovannoni SJ. (2002). High-Throughput Methods for Culturing Microorganisms in Very-Low-Nutrient Media Yield Diverse New Marine Isolates. *Appl Environ Microbiol* **68**: 3878–3885.
4. Dykxma S, Bischof K, Fuchs BM, Hoffmann K, Meier D, Meyerdierks A, *et al.* (2016). Ubiquitous Gammaproteobacteria dominate dark carbon fixation in coastal sediments. *ISME J* **10**: 1–15.
5. Francis CA, Beman JM, Kuypers MMM. (2007). New processes and players in the nitrogen cycle: the microbial ecology of anaerobic and archaeal ammonia oxidation. *Isme J* **1**: 19–27.
6. Glaubitz S, Kießlich K, Meeske C, Labrenz M, Jürgens K. (2013). SUP05 Dominates the gammaproteobacterial sulfur oxidizer assemblages in pelagic redoxclines of the central Baltic and Black seas. *Appl Environ Microbiol* **79**: 2767–2776.
7. Hawley AK, Brewer HM, Norbeck AD, Pasa-Tolic L, Hallam SJ. (2014). Metaproteomics reveals differential modes of metabolic coupling among ubiquitous oxygen minimum zone microbes. *Proc Natl Acad Sci* **111**: 11395–11400.
8. Lam P, Kuypers MMM. (2011). Microbial nitrogen cycling processes in oxygen minimum zones. *Ann Rev Mar Sci* **3**: 317–345.
9. Lavik G, Stuhmann T, Bruchert V, Van der Plas A, Mohrholz V, Lam P, *et al.* (2009). Detoxification of sulphidic African shelf waters by blooming chemolithotrophs. *Nature* **457**: 581–584.
10. Marshall KT, Morris RM. (2012). Isolation of an aerobic sulfur oxidizer from the SUP05/Arctic96BD-19 clade. *ISME J* **7**: 452–455.
11. Mattes TE, Nunn BL, Marshall KT, Proskurowski G, Kelley DS, Kawka OE, *et al.* (2013). Sulfur oxidizers dominate carbon fixation at a biogeochemical hot spot in the dark ocean. *ISME J* **7**: 1–12.

12. Schunck H, Lavik G, Desai DK, Großkopf T, Kalvelage T, Löscher CR, *et al.* (2013). Giant Hydrogen Sulfide Plume in the Oxygen Minimum Zone off Peru Supports Chemolithoautotrophy. *PLoS One* **8**
13. Staley JT, Konopka A. (1985). Microorganisms in Aquatic and Terrestrial Habitats. *Ann Rev Microbiol* 321–46.
14. Stramma L, Johnson GC, Sprintall J, Mohrholz V. (2008). Expanding oxygen-minimum zones in the tropical oceans. *Science* **320**: 655–658.
15. Taylor GT, Iabichella M, Ho TY, Scranton MI, Thunell RC, Muller-Karger F, *et al.* (2001). Chemoautotrophy in the redox transition zone of the Cariaco Basin: A significant midwater source of organic carbon production. *Limnol Oceanogr* **46**: 148–163. Teske A. (2010). Oceans. Cryptic links in the ocean. *Science (80-)* **330**: 1326–7.
16. Ulloa O, Canfield DE, DeLong EF, Letelier RM, Stewart FJ. (2012). Microbial oceanography of anoxic oxygen minimum zones. *Proc Natl Acad Sci U S A* **109**: 15996–6003.
17. Whitman WB, Coleman DC, Wiebe WJ. (1998). Prokaryotes: The unseen majority. *Proc Natl Acad Sci* **95**: 6578–6583.
18. Wright JJ, Konwar KM, Hallam SJ. (2012). Microbial ecology of expanding oxygen minimum zones. *Nat Rev Microbiol* **10**: 381–394.
19. Zaikova E, Walsh DA, Stilwell CP, Mohn WW, Tortell PD, Hallam SJ. (2010). Microbial community dynamics in a seasonally anoxic fjord: Saanich Inlet, British Columbia. *Environ Microbiol* **12**: 172–91.

List of Important Abbreviations

16S SSU rRNA in bacteria and archaea

μM micromolar

nM nanomolar

AOA Ammonia oxidizing archaea

ATP Adenosine triphosphate

BLAST Basic Local Alignment Search Tool

bp base pair

DAPI 4',6-diamidino-2-phenylindole, a fluorescent DNA-binding stain

DMSO Dimethylsulfoxide

DMSP Dimethyl sulfoniopropionate

DNA Deoxyribonucleic acid

DNRA Dissimilatory nitrate reduction to ammonia

DOM Dissolved organic matter

M Molar

NADH Nicotinamide adenine dinucleotide

NESAP Northeast subarctic Pacific Ocean

OMZ Oxygen minimum zone

PCR Polymerase chain reaction

PDO Pacific Decadal Oscillation

POM Particulate organic matter

rRNA Ribosomal ribonucleic acid

SI Saanich Inlet

Chapter 1. THE GENOME OF *THIOGLOBUS AUTOTROPHICUS* STRAIN EF1, A CHEMOAUTOTROPH FROM THE SUP05 CLADE OF MARINE GAMMA-PROTEOBACTERIA

Citation: Shah, V. & Morris, R. M. Genome Sequence of ‘Candidatus Thioglobus autotrophicus’ Strain EF1, a Chemoautotroph from the SUP05 Clade of Marine Gammaproteobacteria. ASM Genome Announc. 3, 6–7 (2015).

1.1 ABSTRACT

Chemoautotrophic marine bacteria from the SUP05 clade often dominate low oxygen waters in upwelling regions, fjords and hydrothermal systems. They are key players in the marine carbon, nitrogen and sulfur cycles. Till date SUP05 have evaded cultivation and thus their complete genomic potential remains unknown. Here I present the complete genome sequence of *Thioglobus autotrophicus* strain EF1, the first cultured chemoautotrophic representative from the SUP05 clade. The genome of “Ca T. autotrophicus” has 1.52 million base pairs, a GC content of 39.1%. and codes for 1,506 proteins, 92 pseudogenes, 3 rRNAs (5S, 16S and 23S) and 35 tRNAs and contains key genes for carbon, nitrogen and sulfur metabolism.

1.2 INTRODUCTION

Chemoautotrophic members of the SUP05 clade of marine gamma-proteobacteria are abundant in the suboxic ocean (Lavik et al 2009, Canfield et al 2010, Zaikova et al 2010).

Chemoautotrophic members of the *sup05* subclade are of particular interest because of their potential to mediate biogeochemical cycles in fjords, upwelling zones and sulfidic regions like

the Black Sea (Hawley et al 2014, Glaubitz et al 2014). Although members of the SUP05 clade have evaded cultivation, cultivation-independent studies suggest that they have critical roles in mediating chemoautotrophic carbon fixation, denitrification, and sulfur oxidation (Wright et al 2012). I isolated the first cultured chemoautotrophic representative from the SUP05 clade; *Candidatus Thioglobus autotrophicus* strain EF1, from a redox gradient in Effingham Inlet, British Columbia to elucidate the roles of chemoautotrophic SUP05 in carbon, nitrogen and sulfur cycling. The complete genome sequence of *T. autotrophicus* is 1,512,449 bp long and has key genes for chemoautotrophy.

1.3 METHODS

1.3.1 DNA extraction

Genomic DNA was extracted from a total of 62 pure cultures grown anaerobically in 100 ml bottles. Cells were grown to early stationary phase ($\sim 2.0 \times 10^6$ cells/ml) and then collected on sterile Supor-200 0.2 μ M polyethersulfone filters (Pall, Port Washington, NY). DNA was extracted using a Qiagen Blood and Tissue kit with modifications as previously described (Marshall & Morris 2013). DNA extracts were checked for purity using 16S rRNA sequence and then pooled into one sample containing 1.3 micrograms of DNA, quantified using Qubit Fluorometric Quantification device (ThermoFisher Scientific, CO, US). DNA was cleaned using a PowerClean Pro DNA cleanup kit (MoBio, MD, US)

1.3.2 DNA sequencing

Clone library preparation for genome sequencing was performed at the University of Washington's Genome Science Department using Pacific Bioscience's single molecule real-time (SMRT) sequencing technology. De novo assembly of the *T. autotrophicus* EF1 genome was conducted using the Hierarchical Genome Assembly Process (HGAP) as previously described (Koren et al 2012). Single reads were mapped to seed reads, a Celera assembler created overlapping consensus sequences, and the remaining inDel (insertion/deletion) and base substitution errors were removed. This method has been found to produce highly accurate, complete de novo assemblies for small prokaryotic genomes (Roberts et al 2013). HGAP assembly of the *T. autotrophicus* EF1 genome resulted in a single contiguous sequence. The complete genome sequence of *T. autotrophicus* EF1 used 100% of cleaned reads with an average coverage of 106x, indicating high confidence in a single circular chromosome 1,512,449 bp in length.

1.3.3 Genome completion using PCR and Annotation

The single contiguous sequence obtained from Pacbio's HGAP assembly was used to design two primers (using Geneious software v 7.1) spanning a single gap. Genomic DNA was amplified using a PCR reaction with primer pair 440F_GSOEF1 (5'- CCCATGCTTTGCGATGTGAC -3') and 1055R_GSOEF1 (5'-CAATCAACACGCGACCTGTC-3'). The PCR reaction was run for 35 cycles at the denaturation temperature of 94 °C for 30 seconds, hybridization temperature of 55 °C for 60 seconds and elongation temperature of 72 °C for 120 seconds. The resulting template was sequenced via Sanger DNA sequencing service provided by GENEWIZ (Seattle, US). The sequence obtained from GENEWIZ was used to create a consensus sequence

connecting the original contig. and forming a circular chromosome. Protein coding sequences were identified and annotated via NCBI's automatic Prokaryotic Genome Annotation Pipeline and were checked against RAST annotations (Aziz et al 2008, Overbeek et al 2014,), IMG annotations (Markowitz et al 2012), and in some cases by phylogenetic analyses. Discrepancies were corrected and final annotations were submitted to NCBI.

1.4 RESULTS

1.4.1 Genetic potential of “*Ca. T. autotrophicus*” strain EF1

The complete genome of “*Ca. T. autotrophicus*” strain EF1 has a GC content of 39.1%. It codes for 1,506 proteins, 92 pseudogenes, 3 rRNAs (5S, 16S and 23S) and 35 tRNAs. It has the genetic potential to grow as a facultatively anaerobic chemolithoautotroph that oxidizes sulfur and can reduce O₂, NO₃⁻ and NO (Figure 1B). The genome codes for key enzymes for carbon fixation via the Calvin-Benson-Bassham (CBB) cycle, including *cbbYCOQR*, carbonic anhydrase and cytochrome *cbb3*, one copy of the small subunit of RuBisCO (form I) and two copies of the large subunit of RuBisCO (form I and form II) (Badger & Bek, 2008). RuBisCO form I is composed of large and small subunits and is present in most chemoautotrophic bacteria, cyanobacteria, red and brown algae and all plants. Form II is a dimer of large subunits and is present in purple non-sulfur bacteria, some chemoautotrophic bacteria and in dinoflagellates. Some non-sulfur phototrophic bacteria contain both forms of RuBisCO. Strain EF1 is facultatively anaerobic and has likely adapted to use form IA RuBisCO or form II RuBisCO, depending on the ratio of CO₂ to O₂. Strain EF1 codes for complete glycolytic and phosphogluconate pathways (nonoxidative), and has most genes encoding the tricarboxylic acid (TCA) cycle. “*Ca. T. autotrophicus*” strain

EF1 does not code for α -ketoglutarate dehydrogenase, a key TCA enzyme that is also missing from closely related symbiont genomes and a planktonic SUP05 population genome from Saanich Inlet (Walsh et al., 2009). The absence of α -ketoglutarate dehydrogenase suggests that “*Ca. T. autotrophicus*” strain EF1 is an obligate autotroph (Wood et al., 2004). Cytochrome c oxidase was also identified, along with a suite of genes for oxidative phosphorylation, further indicating the potential for strain EF1 to grow under aerobic conditions.

Genes for chemoautotrophic energy conservation were also identified. These include genes for inorganic sulfur oxidation (*fccAB*, *dsrABCH*, *aprABM*, *soxABXYZ* and *rhodanese sulfurtransferase*) and for aerobic and anaerobic respiration on O₂, NO₃⁻ and NO (*narQGHII*, *napABGD* and *norBCD*) (Figure 1B). Sulfur oxidation genes confer the ability to oxidize a broad range of reduced sulfur compounds, including hydrogen sulfide (H₂S), elemental sulfur (S⁰) and thiosulfate (S₂O₃²⁻). Similar to Saanich Inlet SUP05, strain EF1 is also missing *soxCD* sulfur dehydrogenase genes, suggesting that they store S⁰. The absence of *soxCD* has coincided with the ability of a closely related symbiont, *Ruthia magnifica*, to store sulfur in the form of extracellular globules (Newton et al., 2007).

Genes for anaerobic respiration confer the ability to carry out two of the four steps associated with sequential denitrification (NO₃⁻ → NO₂⁻ → NO → N₂O → N₂). Strain EF1 has the genetic potential to reduce nitrate to nitrite (NO₃⁻ → NO₂⁻) and to reduce nitric oxide to nitrous oxide (NO → N₂O) (Figure 1B), but lacks genes to reduce nitrite to nitric oxide (NO₂⁻ → NO) or to reduce nitrous oxide to nitrogen gas (N₂O → N₂). Though the ability to use NO₂⁻ and N₂O as terminal electron acceptors has been observed in environmental datasets (Walsh et al., 2009;

Murillo et al., 2014; Hawley et al., 2014;). I found that strain EF1 is missing key genes required to use hydrogen gas (H₂) as an electron donor as previously reported for environmental SUP05 in the Guaymas Basin (Anantharaman et al., 2013). “*Ca. T. autotrophicus*” strain EF1 has key genes required to use either NH₄⁺ or organic nitrogen for biosynthesis (Figure 1). These include genes that confer the ability to regulate intracellular nitrogen and to assimilate NH₄⁺ and amino acids. Strain EF1 codes for two ammonia transporters, NADPH-dependent glutamate synthase (GS) and glutamine oxoglutarate aminotransferase (GOGAT), as well as components of amino acid (AA) and peptide ABC-transporters. The complete genome sequence of *Thioglobus autotrophicus* strain EF1 is available in GenBank under accession number CP010552.

1.5 REFERENCES

1. Sunamura, M, Higashi, Y, Miyako, C, Ishibashi, J, Maruyama, A. 2004. Two bacteria phylotypes are predominant in the Suiyo seamount hydrothermal plume. *Appl. Environ. Microbiol.* 70:1190-1198.
2. Lavik, G, Stuhmann, T, Bruchert, V, Van der Plas, A, Mohrholz, V, Lam, P, Mussmann, M, Fuchs, BM, Amann, R, Lass, U, Kuypers, MM. 2009. Detoxification of sulphidic African shelf waters by blooming chemolithotrophs. *Nature.* 457:581-584.
3. Canfield, DE, Stewart, FJ, Thamdrup, B, De Brabandere, L, Dalsgaard, T, Delong, EF, Revsbech, NP, Ulloa, O. 2010. A Cryptic Sulfur Cycle in Oxygen-Minimum-Zone Waters off the Chilean Coast. *Science.* 330:1375-1378.
4. Beman, JM, Carolan, MT. 2013. Deoxygenation alters bacterial diversity and community composition in the ocean's largest oxygen minimum zone. *Nature Communications.* 4:Article Number: 2705.
5. Hawley, AK, Brewer, HM, Norbeck, AD, Pasa-Tolic, L, Hallam, SJ. 2014. Metaproteomics reveals differential modes of metabolic coupling among ubiquitous oxygen minimum zone microbes. *Proc. Natl. Acad. Sci. U. S. A.* 111:11395-11400.
6. Zaikova, E, Walsh, DA, Stilwell, CP, Mohn, WW, Tortell, PD, Hallam, SJ. 2010. Microbial community dynamics in a seasonally anoxic fjord: Saanich Inlet, British Columbia. *Environ. Microbiol.* 12:172-191.
7. Glaubitz, S, Kiesslich, K, Meeske, C, Labrenz, M, Jurgens, K. 2013. SUP05 dominates the Gammaproteobacterial sulfur oxidizer assemblages in pelagic redoxclines of the central Baltic and Black Seas. *Appl. Environ. Microbiol.* 79:2767-2776.

8. Walsh, DA, Zaikova, E, Howes, CG, Song, YC, Wright, JJ, Tringe, SG, Tortell, PD, Hallam, SJ. 2009. Metagenome of a versatile chemolithoautotroph from expanding oceanic dead zones. *Science*. 326:578-582
9. Mattes, TE, Nunn, BL, Marshall, KT, Proskurowski, G, Kelley, DS, Kawka, OE, Goodlett, DR, Hansell, DA, Morris, RM. 2013. Sulfur oxidizers dominate carbon fixation at a biogeochemical hot spot in the dark ocean. *Isme j*. 7:2349-2360.
10. Hawley, AK, Brewer, HM, Norbeck, AD, Pasa-Tolic, L, Hallam, SJ. 2014. Metaproteomics reveals differential modes of metabolic coupling among ubiquitous oxygen minimum zone microbes. *Proc. Natl. Acad. Sci. U. S. A.* 111:11395-11400.
11. Marshall, KT, Morris, RM. 2013. Isolation of an aerobic sulfur oxidizer from the SUP05/Arctic96BD-19 clade. *Isme j*. 7:452-455.
12. Koren, S, Schatz, MC, Walenz, BP, Martin, J, Howard, JT, Ganapathy, G, Wang, Z, Rasko, DA, McCombie, WR, Jarvis, ED. 2012. Hybrid error correction and de novo assembly of single-molecule sequencing reads. *Nat. Biotechnol.* 30:693-700.
13. Roberts, RJ, Carneiro, MO, Schatz, MC. 2013. The advantages of SMRT sequencing. *Genome Biol.* 14:405.
14. Aziz, RK, Bartels, D, Best, AA, DeJongh, M, Disz, T, Edwards, RA, Formsma, K, Gerdes, S, Glass, EM, Kubal, M, Meyer, F, Olsen, GJ, Olson, R, Osterman, AL, Overbeek, RA, McNeil, LK, Paarmann, D, Paczian, T, Parrello, B, Pusch, GD, Reich, C, Stevens, R, Vassieva, O, Vonstein, V, Wilke, A, Zagnitko, O. 2008. The RAST Server: rapid annotations using subsystems technology. *BMC Genomics*. 9:75-2164-9-75.
15. Overbeek, R, Olson, R, Pusch, GD, Olsen, GJ, Davis, JJ, Disz, T, Edwards, RA, Gerdes, S, Parrello, B, Shukla, M, Vonstein, V, Wattam, AR, Xia, F, Stevens, R. 2014. The SEED and

the Rapid Annotation of microbial genomes using Subsystems Technology (RAST).
Nucleic Acids Res. 42:D206-14.

16. Markowitz, VM, Chen, IM, Palaniappan, K, Chu, K, Szeto, E, Grechkin, Y, Ratner, A, Jacob, B, Huang, J, Williams, P, Huntemann, M, Anderson, I, Mavromatis, K, Ivanova, NN, Kyrpides, NC. 2012. IMG: the Integrated Microbial Genomes database and comparative analysis system. Nucleic Acids Res. 40:D115-22.
17. Anantharaman, K., Breier, J. A., Sheik, C. S. & Dick, G. J. 2013. Evidence for hydrogen oxidation and metabolic plasticity in widespread deep-sea sulfur-oxidizing bacteria. *Proc. Natl. Acad. Sci. U. S. A.* **110**, 330–5

Figure 1.1 Circular representation of the “*Ca. T. autotrophicus*” strain EF1 complete genome. Innermost circle - GC skew (purple is negative skew and green is positive skew). Bars within solid lines indicate predicted coding regions colored by metabolic categories. Orange (S-oxidation and reduction genes): *sox* (sulfur oxidation), *apr* (adenosine-5-phosphate reductase), *fcc* (flavocytochrome c sulfide dehydrogenase), and *dsr* (dissimilatory sulfite reductase). Navy (NO₃⁻ and NO reduction genes): *nap* (periplasmic nitrate reductase), *nar* (nitrate reductase), *nor* (nitric oxide reductase). Teal (exogenous N assimilation): GOGAT (glutamate synthase) and ammonia, amino acid, and peptide transporters. Red (CO₂ fixation): *rbcS* (RuBisCO small subunit), *rbcL* (RuBisCO large subunit).

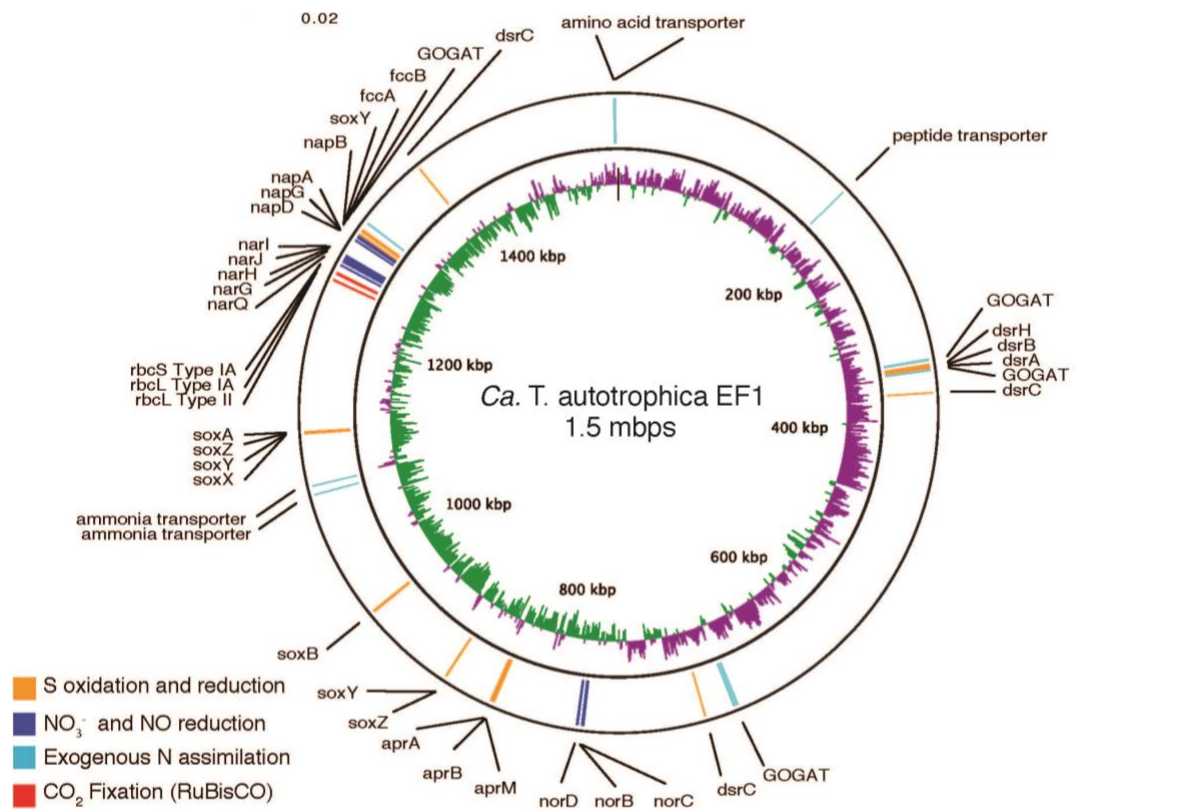


Table 1.1. Metadata associated with the Pacific Biosciences sequencing pipeline and with the Hierarchical Genome Assembly Process (HGAP).

| | |
|---------------------------------|-----------------|
| SMRT Cell | 1 |
| Library Preparation | 20 kbp shearing |
| Library Size Range | 3-20 kbp |
| Number of Bases | 198082549 |
| Number of Reads | 37021 |
| N50 Read Length | 8588 |
| Mean Read Length | 5350 |
| Mapped Reads | 30150 |
| Mapped Read Length of Insert | 3363 |
| Reference Length | 1512379 |
| Bases Called | 100% |
| Reference Consensus Concordance | 99.9979 |
| Average Coverage | 105.88 |
| Polished Contigs | 1 |
| Polished Contig Length | 1512413 |

Chapter 2. CULTIVATION OF A CHEMOAUTOTROPH FROM THE SUP05 CLADE OF MARINE BACTERIA THAT PRODUCES NITRITE AND CONSUMES AMMONIA

Citation: Shah, V., Chang, B. X. & Morris, R. M. Cultivation of a chemoautotroph from the SUP05 clade of marine bacteria that produces nitrite and consumes ammonium. ISME J. 11, 1–9 (2017)

2.1 ABSTRACT

Marine oxygen minimum zones (OMZs) are expanding regions of intense nitrogen cycling. Up to half of the nitrogen available for marine organisms is removed from the ocean in these regions. Metagenomic studies have identified an abundant group of sulfur-oxidizing bacteria (SUP05) with the genetic potential for nitrogen cycling and loss in OMZs. However, SUP05 have defied cultivation and their physiology remains untested. I cultured, sequenced and tested the physiology of an isolate from the SUP05 clade. I describe a facultatively anaerobic sulfur-oxidizing chemolithoautotroph that produces nitrite and consumes ammonium under anaerobic conditions. Genetic evidence that closely related strains are abundant at nitrite maxima in OMZs suggests that sulfur-oxidizing chemoautotrophs from the SUP05 clade are a potential source of nitrite, fueling competing nitrogen removal processes in the ocean.

2.2 INTRODUCTION

Nitrogen is a limiting nutrient in much of the world's ocean. Thirty to fifty percent of the fixed nitrogen available for marine organisms is lost from the ocean due to the biological production of

dinitrogen gas (N_2) in oxygen minimum zones (OMZs) (Codispoti et al., 2001; Galloway et al., 2008). Nitrogen loss in these regions is attributed to two microbially mediated processes, heterotrophic denitrification (Jayakumar et al., 2004; Castro-Gonzalez et al., 2005; Ward et al., 2009; Babbin et al., 2014) and anaerobic ammonia oxidation (anammox) (Kuypers et al., 2005; Thamdrup et al., 2006; Hamersley et al., 2007; Lam et al., 2009). Genomic data have identified an abundant group of sulfur-oxidizing marine chemoautotrophs (SUP05) that are assumed to contribute to either denitrification or anammox (Walsh et al., 2009; Canfield et al., 2010; Zaikova et al., 2010; Ulloa et al., 2012; Wright et al., 2012; Mattes et al., 2013; Murillo et al., 2014; Hawley et al., 2014). Members of the SUP05 clade are hypothesized to contribute directly by sequential reduction of nitrate (NO_3^-) to nitrogenous gases (N_2O or N_2), or indirectly by dissimilative NO_3^- reduction to ammonia (DNRA), which can in turn fuel anammox (Walsh et al., 2009; Canfield et al., 2010; Murillo et al., 2014; Hawley et al., 2014).

SUP05 also have the genetic potential to produce nitrite (NO_2^-), which is a critical intermediate in denitrification and a necessary reductant for anammox. The sources of NO_2^- , and in particular the secondary NO_2^- maximum, in OMZs are poorly understood (Lam et al., 2009).

Accumulation of NO_2^- in OMZs has been attributed to heterotrophic denitrification leading to N-loss (Lam et al., 2011). The current paradigm is that NO_2^- in OMZs is produced at the oxycline by aerobic ammonia oxidizing archaea and bacteria (AOA, AOB) (Hawley et al., 2014) and within the OMZ by heterotrophs (Codispoti et al., 2001; Francis et al., 2007; Lam et al., 2011). Chemoautotrophic SUP05 also have the genetic potential to respire NO_3^- and produce NO_2^- (Walsh et al., 2009; Murillo et al., 2014; Hawley et al., 2014). Here I test the hypothesis that a

chemoautotrophic bacterium from the SUP05 clade has the potential to contribute to the NO_2^- maximum in OMZs by respiring NO_3^- and producing NO_2^- .

I isolated a representative from the SUP05 clade to elucidate the effects of these sulfur-oxidizing bacteria on the marine nitrogen cycle. Here I describe the isolation, genetic potential and growth requirements of a sulfur-oxidizing chemolithoautotroph that produces NO_2^- and is limited by ammonium (NH_4^+). I provide insights into the hypothesized roles of SUP05 in the marine nitrogen cycle that could not be inferred from environmental sequence data alone. Our findings suggest that SUP05 produce NO_2^- , a critical intermediate required for nitrogen removal processes (anammox and denitrification).

I propose the following name for the first isolate from the SUP05 clade:

Thioglobus gen. (Marshall & Morris, 2013)

“*Candidatus Thioglobus autotrophicus*” sp. nov

Etymology: au.to.tro'phi.ca. Gr. n. *autos* self; Gr. adj. *trophikos* nursing, tending or feeding; N.L. fem. adj. *autotrophicus* autotroph

2.3 MATERIALS AND METHODS

2.3.1 *Cultivation*

Water was collected from Effingham Inlet (49°04.2685' N, 125°09.4270' W) during a research cruise aboard the R/V *Thomas G. Thompson* in February 2013 using a rosette with 10 liter Niskin bottles and equipped with a Seabird conductivity, temperature and density (CTD) device and dissolved oxygen (DO) sensors calibrated by Winkler titrations. Live cells were collected

from the top of the suboxic zone (defined as the minimum value obtained by the Seabird DO sensor) (Supplementary Figure 1). Cell numbers were estimated based on prior results and diluted to extinction (5 cells/well) in two 96 well Teflon plates (SonomaTesting, Santa Rosa, CA) using a high throughput culture method with on-site filter sterilized seawater (30 kD) used as media. One 96 well plate was enriched with 1 mM thiosulfate ($S_2O_3^{2-}$) while the other was used as a control and contained only filter sterilized seawater. Growth in each well was measured every 7 days in incubations at *in situ* temperatures (10 °C) by first transferring 150 μ l aliquots of culture into 96 well polycarbonate plates (Millipore, Billerica, MA) and then staining each well with SYBR Green I (Invitrogen, Carlsbad, CA) diluted in TRIS buffer pH 7.4 at a final concentration of 1/2000. Cell concentrations in 96 well polycarbonate plates were measured using an Easyflow Guava flow cytometer equipped with a 96 well plate reader (Millipore, Billerica, MA).

2.3.2 *Isolate identification*

Cultures were identified as previously described (Marshall & Morris, 2013), with the following modifications. Cells were transferred to 250 ml acid washed polycarbonate flasks (10% HCl) and grown to early stationary phase ($\sim 2.0 \times 10^6$ cells/ml), then collected on sterile Supor-200 0.2 μ m polyethersulfone filters (Pall, Port Washington, NY). I identified cultures by amplifying and sequencing the 16S rRNA gene with bacterial primers (27F, 519F/R, 926F/R and 1492R). Sequences were subsequently aligned with nearly complete 16S rRNA gene sequences and a maximum likelihood tree was constructed using RAxML. *Methylococcus sp.* strain Texas was used as an out-group and 100 bootstrap replicates were used to evaluate clusters (Figure 1A). Culture purity was verified using terminal restriction fragment length polymorphism (TRFLP)

analyses. Briefly, universal primers 27F and 1492R were used to amplify 16S DNA that was then restricted with either MboI or HaeIII (New England Biolabs) as previously described (Marshall & Morris, 2013).

2.3.3 *Growth conditions*

T. autotrophicus EF1 cells were grown at *in situ* temperatures (10 °C) in acid-washed (10% HCl) and autoclaved bottles containing copiotrophic seawater media from Puget Sound or oligotrophic seawater media from the Sargasso Sea (Supplementary Table 2). Aerobic cultures were maintained in acid washed polycarbonate bottles. Anaerobic cultures were maintained in acid washed and autoclaved 125 ml serum bottles, sealed with 20 mm butyl rubber stoppers (Wheaton), then bubbled with an N₂:CO₂ gas mix (1000 ppm CO₂, Praxair Specialty Gas Mix) for 10 minutes, and headspace sparged for an additional 5 minutes. Complete removal of oxygen inside serum bottles was confirmed using BD GasPak™ Anaerobic strips added to an uninoculated control serum bottle. Experiments (aerobic and anaerobic) were started by transferring 1000 cells in early exponential growth phase to new media. Culture purity was checked before and after each physiology study by sequence analysis and TRFLP.

2.4 RESULTS AND DISCUSSION

2.4.1 *Isolation of a representative from the SUP05 clade*

Six out of 192 culture wells inoculated with water from a redox gradient in Effingham Inlet were positive for growth after 21 days. Four of the cultures had identical 16S rRNA gene sequences and were identified as members of the SUP05 clade. One culture was identified as a closely

related gammaproteobacteria just outside the clade and one culture was identified as an epsilon-proteobacteria related to *Arcobacter sp.* associated with marine sponges. All are suspected sulfur-oxidizing bacteria. “*Ca. T. autotrophicus*” strain EF1 was selected for further study. The remaining cultures were cryopreserved.

Phylogenetic analysis and genome sequencing further confirmed the identity and genetic potential of “*Ca. T. autotrophicus*” strain EF1 (Figure 1). Strain EF1 is most closely related to sequences from the original SUP05 clade described by Walsh et al., (2009). These include environmental clones recovered from a broad range of OMZs and symbionts of deep-sea mollusk *Bathymodiolus sp.* Related sequences derived from the whole genomes of symbionts, and from environmental clones from the northeast Pacific ridge (Huber et al., 2006), the Namibian upwelling system (Lavik et al., 2009), Suiyo Seamount (Sunamara et al., 2004), Saanich Inlet (Walsh et al., 2009), the Eastern North Pacific and Eastern South Pacific (Stevens & Ulloa, 2008), the South Atlantic and North Pacific Gyres (Swan et al., 2011) and Puget Sound (Marshall & Morris, 2013). The complete 16S rRNA gene sequences obtained from the “*Ca. T. singularis*” strain PS1 and “*Ca. T. autotrophicus*” strain EF1 genomes were also analyzed using the SILVA high quality ribosomal RNA database (Quast et al., 2012). “*Ca. T. singularis*” strain PS1 was most closely related to sequences in the Arctic96BD-19 subclade (ZD0405 in SILVA). “*Ca. T. autotrophicus*” strain EF1 was most closely related to sequences in the SUP05 subclade.

The purity of “*Ca. T. autotrophicus*” strain EF1 was confirmed by several methods. TRFLP analyses identified a single 266 bp fragment using the restriction enzyme MboI and a 193 bp fragment using the restriction enzyme HaeIII (Supplementary Figure 2). These exactly match

the fragments predicted from the 16S rRNA gene sequence. No other fragments were observed. Purity was further confirmed by quantitative fluorescence *in situ* hybridization (FISH) analyses with a SUP05 specific probe (GSO-1032) that exactly matches the 16S rRNA (Glaubitz et al., 2013) (Supplementary Figure 2). All of the DAPI stained objects observed in three images (117/115/118) also hybridized to the SUP05 probe (total = 350/350). Cultures were subsequently cryopreserved and revived from glycerol stocks several times and under both aerobic and anaerobic growth conditions. Sequence and restriction analyses were used to check purity every time a culture was revived from glycerol stocks and before and after every physiology experiment. In every case, these analyses produced the same 16S rRNA gene sequences and the same restriction patterns. Transmission electron microscopy images revealed a single morphology, indicating that strain EF1 is a small (~0.3-0.4 μm) cocci shaped bacterium that produces extracellular globules resembling those produced by “*Ca. T. singularis*” PS1 (Supplementary Figure 3).

2.4.2 *Growth requirements*

Physiology experiments confirmed that strain EF1 is a facultatively anaerobic chemolithoautotroph that requires inorganic sulfur as a source of electrons (Figure 2). Batch cultures grew to an average final cell density of 3.6×10^6 cells/ml under aerobic conditions in seawater media containing 1 mM $\text{S}_2\text{O}_3^{2-}$ and to an average final cell density of 2.8×10^6 cells/ml under anaerobic conditions in seawater media amended with 1 mM $\text{S}_2\text{O}_3^{2-}$, 100 μM of NO_3^- and sparged with a mixture of $\text{N}_2:\text{CO}_2$ (Figure 2A and B, respectively). Cells were unable to grow in aerobic seawater media that lacked $\text{S}_2\text{O}_3^{2-}$ or in anaerobic media that lacked either $\text{S}_2\text{O}_3^{2-}$ or CO_2 . This indicates that “*Ca. T. autotrophicus*” strain EF1 requires a reduced form of inorganic sulfur

for electrons and CO₂ for biosynthesis. I have found that strain EF1 cells survive two transfers with no additional sulfur and that they contain extracellular globules (Supplementary Figure 3). This is likely due to their potential to store sulfur in extracellular globules (Walsh et al., 2009; Marshall & Morris, 2013; Hawley et al., 2014). No growth was observed when “*Ca. T. autotrophicus*” strain EF1 was grown with H₂ as an electron donor (Supplementary Figure 4).

I grew strain EF1 on copiotrophic media (Supplementary Table 2) enriched with NO₃⁻ to further evaluate its potential for dissimilatory NO₃⁻ reduction under anaerobic conditions (Figure 3). Cultures grew to similar cell densities at *in situ* concentrations of NO₃⁻ (32 μM) and when 100 μM of additional NO₃⁻ was added to the media (Figure 3A). Strain EF1 was not limited by NO₃⁻ on copiotrophic seawater media. In both cases there was strong evidence for dissimilatory NO₃⁻ reduction, as indicated by a 1:1 conversion of NO₃⁻ to NO₂⁻ (Figure 3B), as well as uptake of NH₄⁺ (Figure 3C) and an increase in the production of N₂O (Figure 3D). Although NO was not added to the media, some NO may have been present in the seawater used to make the media or introduced into as a contaminant via the N₂:CO₂ gas mix used to sparge the media. Regardless, growth experiments support genomic predictions and previously published results from the field indicating that SUP05 produce N₂O (Walsh et al., 2009; Hawley et al., 2014). EF1 cells did not produce N₂ gas (Supplementary Figure 4).

The potential for “*Ca. T. autotrophicus*” strain EF1 to respire NO₃⁻ and assimilate NH₄⁺ was evaluated further under nitrogen limitation using oligotrophic seawater media (Figure 4, Supplementary Table 2). Cultures grew to the highest final cell densities (average 1.2x10⁶ cells/ml) in media that was amended with 1 mM S₂O₃²⁻, 100 μM NO₃⁻ and 5 μM NH₄⁺ (Figure

4A). Cells grew to lower cell densities (average 6.2×10^5 cells/ml) and had slower growth rates when only $\text{S}_2\text{O}_3^{2-}$ and NO_3^- were added to the media. There was a 1:1 conversion of NO_3^- to NO_2^- in treatments amended with $\text{S}_2\text{O}_3^{2-}$ and NO_3^- , or with $\text{S}_2\text{O}_3^{2-}$, NO_3^- and NH_4^+ (Figure 4B). The amount of NO_3^- converted to NO_2^- increased four-fold (average increase from 5 μM to 22 μM) when NH_4^+ was added to the media and there was a decrease in NH_4^+ concentration over time (Figure 4B). Some growth was observed in $\text{S}_2\text{O}_3^{2-}$ only controls. This is likely due to the low concentrations of NO_3^- (0.15 μM) and NH_4^+ (0.04 μM) present in oligotrophic seawater media (Supplementary Table 2). This experiment further confirmed that “*Ca. T. autotrophicus*” strain EF1 was unable to use NO_2^- as a terminal electron acceptor (Figure 4C and 4D). When cells were amended with NO_2^- instead of NO_3^- , no difference in growth was observed between amendments and controls. NO_2^- and NH_4^+ concentrations remain unchanged throughout the experiment. The potential to assimilate amino acids (Promega Amino Acid Mixture) in oligotrophic seawater was also tested. Cultures were grown in media amended with 1 mM $\text{S}_2\text{O}_3^{2-}$, 100 μM NO_3^- and an amino acid mixture (5 μM of N) (Supplementary Figure 4). There was no discernable difference between cultures amended with amino acids and unamended controls, indicating that strain EF1 prefers NH_4^+ for biogenic nitrogen.

2.4.3 Roles in the marine nitrogen cycle

Evidence that cultured SUP05 produce NO_2^- suggests that related strains are a potential source of NO_2^- in OMZs. There is strong molecular evidence indicating that environmental SUP05 are capable of mediating sequential steps in denitrification. Because these environmental sequence data provide a fragmented view of a population of cells, it is also possible that different SUP05 cells carry out different steps in denitrification, depending on the diversity of SUP05 in a

population, on the concentrations of substrates, and on the range of interactions within a community. Genetic and physiology data from this study suggests that a single strain of SUP05 carries out two non-sequential steps in denitrification. Both cultivation-dependent and cultivation-independent data indicate that the first step in denitrification (NO_3^- reduction to NO_2^-) is highly conserved (Walsh et al., 2009; Canfield et al., 2010; Murillo et al., 2014; Hawley et al., 2014), while the potential to carry out subsequent steps in denitrification are not always identified (Murillo et al., 2014). In addition, SUP05 are often most abundant in areas where NO_2^- accumulates (Canfield et al., 2010; Murillo et al., 2014; Hawley et al., 2014). Glaubitz and colleagues (2013) reported that there was a positive correlation between SUP05 and nitrite concentrations in the Black Sea. Although heterotrophic NO_3^- respiration is currently considered the primary process leading to NO_2^- accumulation within OMZs, there is ample genetic and physiological data suggesting that sulfur-oxidizing chemoautotrophs from the SUP05 clade are a potential source of NO_2^- fueling competing nitrogen removal processes in the ocean.

“*Ca. T. autotrophicus*” strain EF1 growth was also limited by NH_4^+ . In the mid 1950s, Baalsrud and Baalsrud, and van Niel found that the S-oxidizing and NO_3^- -reducing bacterium *Thiobacillus denitrificans* required NH_4^+ or amino acids for biosynthesis (Baalsrud & Baalsrud, 1954; van Niel, 1955). Genes for NH_4^+ transport and amino acid assimilation were identified in the strain EF1 genome and in a SUP05 metagenome assembled from Saanich Inlet (Walsh et al., 2009). They were also expressed by SUP05 in Saanich Inlet and the Southern Ocean (Hawley et al., 2014; Wilkins et al., 2013). The biogenic nitrogen requirement of strain EF1 is low. For example, if “*Ca. T. autotrophicus*” strain EF1 cells have 10 fg of carbon/cell and are at Redfield ratios for carbon and nitrogen (106:16), I estimate that they required $\sim 0.22 \mu\text{M}$ of nitrogen for

biosynthesis in cultures grown on natural seawater media (Figure 3, Figure 4). By comparison, they reduced $\sim 30 \mu\text{M}$ of NO_3^- to $\sim 30 \mu\text{M}$ NO_2^- during respiration. There was no evidence that they respired NO_2^- or that they used amino acids instead of NH_4^+ for biosynthesis (Supplementary Figure 4B). These data support the conclusion that strain EF1 requires relatively high concentrations of NO_3^- for respiration and relatively low concentrations of NH_4^+ for biosynthesis.

“*Ca. T. autotrophicus*” strain EF1 also produced N_2O . Members of the SUP05 bacteria expressed genes to produce N_2O in regions of significant N_2O cycling and emission (Codispoti et al., 2001). A recent study by Babbin and colleagues (Babbin et al., 2015) suggests that rapid N_2O cycling in the suboxic ocean could lead to future increases in N_2O emissions. Environmental sequence data indicate that SUP05 are broadly distributed and abundant in these regions. Growth experiments support field expression data, suggesting that N_2O producing chemoautotrophic SUP05 have important roles in biologically driven nitrogen loss from the ocean (Walsh et al., 2009; Murillo et al., 2014; Hawley et al., 2014).

2.5 CONCLUSION

Data resulting from the cultivation of “*Ca. T. autotrophicus*” strain EF1 have expanded the roles of SUP05 in the marine nitrogen cycle. They suggest that SUP05 are a potential source of NO_2^- and sink for NH_4^+ in anoxic marine waters. In the conceptual metabolic coupling model of an OMZ proposed by Hawley and colleagues (2014), ammonia-oxidizing archaea are the source of NO_2^- in the upper and lower oxycline and SUP05 are the hypothesized source of NH_4^+ at and below the lower oxycline. If under the right conditions SUP05 produce NO_2^- , then elevated

concentrations of NH_4^+ are not required to account for the elevated NO_2^- concentrations at and below the lower oxycline. There is strong evidence indicating that NO_3^- reduction is an independent process that can account for a significant fraction of NO_2^- accumulation in OMZs (Nicholas et al., 2007; Lam et al., 2011). I hypothesize that SUP05 contribute to the secondary NO_2^- maxima when NO_3^- fluxes are relatively high, ammonia concentrations are relatively low and oxygen concentrations fall below $4 \mu\text{M}$. Our calculations suggest that SUP05 would use $\sim 7.3 \text{ nM}$ of NH_4^+ for every μM of NO_2^- produced. This is in stark contrast to ammonia-oxidation and suggests that chemoautotrophic members of the SUP05 clade are an important source of NO_2^- in OMZs.

2.6 REFERENCES

1. Anantharaman K, Breier JA, Sheik CS, Dick GJ. (2013). Evidence for hydrogen oxidation and metabolic plasticity in widespread deep-sea sulfur-oxidizing bacteria. *Proc Natl Acad Sci* 110:330–335.
2. Baalsrud K, Baalsrud K. (1954). Studies on *Thiobacillus denitrificans*. *Arch Mikrobiol* 62:34–62.
3. Babbin AR, Bianchi D, Jayakumar A, Ward BB. (2015). Rapid nitrous oxide cycling in the suboxic ocean. *Science*. 348:1127–1130.
4. Babbin AR, Keil RG, Devol AH, Ward BB. (2014). Oxygen Control Nitrogen Loss in the Ocean. *Science*. 406:406–408.
5. Badger MR, Bek EJ. (2008). Multiple Rubisco forms in proteobacteria: Their functional significance in relation to CO₂ acquisition by the CBB cycle. *J Exp Bot* 59:1525–1541.
6. Canfield DE, Stewart FJ, Thamdrup B, De Brabandere L, Dalsgaard T, Delong EF, *et al.* (2010). A cryptic sulfur cycle in oxygen-minimum-zone waters off the Chilean coast. *Science*. 330:1375–8.
7. Castro-Gonzalez M, Braker G, Farias L, Ulloa O. (2005). Communities of nirS-type denitrifiers in the water column of the oxygen minimum zone in the eastern South Pacific. *Environ Microbiol* 7:1298–1306.
8. Codispoti LA, Brandes JA, Christensen JP, Devol A, Naqvi SWA, Paerl HW, *et al.* (2001). The oceanic fixed nitrogen and nitrous oxide budgets : Moving targets as I enter the anthropocene? *Sci Mar* 65:85–105.
9. Francis CA, Beman JM, Kuypers MMM. (2007). New processes and players in the nitrogen cycle: the microbial ecology of anaerobic and archaeal ammonia oxidation. *ISME J* 1:19–27.

10. Galloway JN, Townsend AR, Erisman JW, Bekunda M, Cai Z, Freney JR, *et al.* (2008). Transformation of the nitrogen cycle: recent trends, questions, and potential solutions. *Science*. **320**:889–892.
11. Georges AA, El-Swais H, Craig SE, Li WK, Walsh DA. (2014). Metaproteomic analysis of a winter to spring succession in coastal northwest Atlantic Ocean microbial plankton. *ISME J* **8**:1301–1313.
12. Glaubitz S, Kießlich K, Meeske C, Labrenz M, Jürgens K. (2013). SUP05 Dominates the Gammaproteobacterial Sulfur Oxidizer Assemblages in Pelagic Redoxclines of the Central Baltic and Black Seas. *Appl Environ Microbiol* **79**:2767–76.
13. Hamersley MR, Lavik G, Woebken D, Rattray JE, Lam P, Hopmans EC, *et al.* (2007). Anaerobic ammonium oxidation in the Peruvian oxygen minimum zone. *Limnol Ocean* **52**:923–933.
14. Hawley AK, Brewer HM, Norbeck AD, Paša-Tolić L, Hallam SJ. (2014). Metaproteomics reveals differential modes of metabolic coupling among ubiquitous oxygen minimum zone microbes. *Proc Natl Acad Sci* **111**:11395–11400.
15. Huber JA, Johnson HP, Butterfield DA, Baross JA. (2006). Microbial life in ridge flank crustal fluids. *Environ Microbiol* **8**:88–99.
16. Jayakumar DA, Francis CA, Naqvi SWA, Ward BB. (2004). Diversity of nitrite reductase genes (*nirS*) in the denitrifying water column of the coastal Arabian Sea. *Aquat Microb Ecol* **34**:69–78.
17. Koren S, Schatz MC, Walenz BP, Martin J, Howard JT, Ganapathy G, *et al.* (2012). Hybrid error correction and de novo assembly of single-molecule sequencing reads. *Nat Biotechnol* **30**:693–700.

18. Kuypers MMM, Lavik G, Woebken D, *et al.* (2005). Massive nitrogen loss from the Benguela upwelling system through anaerobic ammonium oxidation. *Proc Natl Acad Sci U S A* **102**:6478–83.
19. Lam P, Lavik G, Jensen MM, van de Vossenberg J, Schmid M, Woebken D, *et al.* (2009). Revising the nitrogen cycle in the Peruvian oxygen minimum zone. *Proc Natl Acad Sci* **106**:4752–7.
20. Lavik G, Stührmann T, Brüchert V, Van der Plas A, Mohrholz V, Lam P, *et al.* (2009). Detoxification of sulphidic African shelf waters by blooming chemolithotrophs. *Nature* **457**:581–4.
21. Marshall KT, Morris RM. (2013). Isolation of an aerobic sulfur oxidizer from the SUP05/Arctic96BD-19 clade. *ISME J* **7**:452–5.
22. Mattes TE, Nunn BL, Marshall KT, Proskurowski G, Kelley DS, Kawka OE, *et al.* (2013). Sulfur oxidizers dominate carbon fixation at a biogeochemical hot spot in the dark ocean. *ISME J* **7**:2349–2360.
23. Murillo AA, Ramírez-Flandes S, DeLong EF, Ulloa O. (2014). Enhanced metabolic versatility of planktonic sulfur-oxidizing γ -proteobacteria in an oxygen-deficient coastal ecosystem. *Front Mar Sci* **1**:1–13.
24. Nagata T. (1986). Carbon and nitrogen content of natural planktonic bacteria. *Appl Environ Microbiol* **52**:28–32.
25. Newton ILG, Woyke T, Auchtung T a, Dilly GF, Dutton RJ, Fisher MC, *et al.* (2007). The *Calyptogena magnifica* chemoautotrophic symbiont genome. *Science* **315**:998–1000.
26. Niel C van. (1955). Natural Selection in the Microbial World. *J Gen Microbiol* **13**:201–217.

27. Quast C, Pruesse E, Yilmaz P, Gerken J, Schweer T, Yarza P, *et al.* (2013). The SILVA ribosomal RNA gene database project: Improved data processing and web-based tools. *Nucleic Acids Res* **41**:590–596.
28. Roberts RJ, Carneiro MO, Schatz MC. (2013). The advantages of SMRT sequencing. *Genome Biol* **14**:405.
29. Shah V, Morris RM. (2015). Genome Sequence of "Candidatus *Thioglobus autotrophicus*" Strain EF1, a Chemoautotroph from the SUP05 Clade of Marine Gammaproteobacteria. *ASM Genome Announc* **3**:6–7.
30. Stevens H, Ulloa O. (2008). Bacterial diversity in the oxygen minimum zone of the eastern tropical South Pacific. *Environ Microbiol* **10**:1244–1259.
31. Stewart FJ. (2011). Dissimilatory sulfur cycling in oxygen minimum zones: an emerging metagenomics perspective. *Biochem Soc Trans* **39**:1859–1863.
32. Sunamura M, Higashi Y, Miyako C, Ishibashi JI, Maruyama A. (2004). Two Bacteria Phylotypes Are Predominant in the Suiyo Seamount Hydrothermal Plume. *Appl Environ Microbiol* **70**:1190–1198.
33. Swan BK, Martinez-Garcia M, Preston CM, Sczyrba A, Woyke T, Lamy D, *et al.* (2011). Potential for chemolithoautotrophy among ubiquitous bacteria lineages in the dark ocean. *Science*. **333**:1296–300.
34. Thamdrup B, Dalsgaard T, Jensen MM, Ulloa O, Farias L, Escribano R. (2006). Anaerobic ammonium oxidation in the oxygen-deficient waters off northern Chile. *Limnol Ocean* **51**:2145–2156.
35. Ulloa O, Canfield DE, DeLong EF, Letelier RM, Stewart FJ. (2012). Microbial oceanography of anoxic oxygen minimum zones. *Proc Natl Acad Sci* **109**:15996–6003.

36. Walsh DA, Zaikova E, Howes CG, Song YC, Wright JJ, Tringe SG, *et al.* (2009). Metagenome of a versatile chemolithoautotroph from expanding oceanic dead zones. *Science*. **326**:578–82.
37. Ward BB, Devol a H, Rich JJ, Chang BX, Bulow SE, Naik H, *et al.* (2009). Denitrification as the dominant nitrogen loss process in the Arabian Sea. *Nature* **461**:78–81.
38. Wilkins D, Lauro FM, Williams TJ, Demaere MZ, Brown MV, Hoffman JM, *et al.* (2013). Biogeographic partitioning of Southern Ocean microorganisms revealed by metagenomics. *Environ Microbiol* **15**:1318–1333.
39. Wood AP, Aurikko JP, Kelly DP. (2004). A challenge for 21st century molecular biology and biochemistry: What are the causes of obligate autotrophy and methanotrophy? *FEMS Microbiol Rev* **28**:335–352.
40. Wright JJ, Konwar KM, Hallam SJ. (2012). Microbial ecology of expanding oxygen minimum zones. *Nat Rev Microbiol* **10**:381–94.
41. Zaikova E, Walsh DA, Stilwell CP, Mohn WW, Tortell PD, Hallam SJ. (2010). Microbial community dynamics in a seasonally anoxic fjord: Saanich Inlet, British Columbia. *Environ Microbiol* **12**:172–91.

Figure 2.1. Maximum likelihood tree of marine gamma sulfur-oxidizing bacteria 16S rRNA sequences. The tree was constructed using RAxML. Bootstrap values >40 are labeled at nodes (100 iterations). Red are symbionts, green are clones and black are isolates

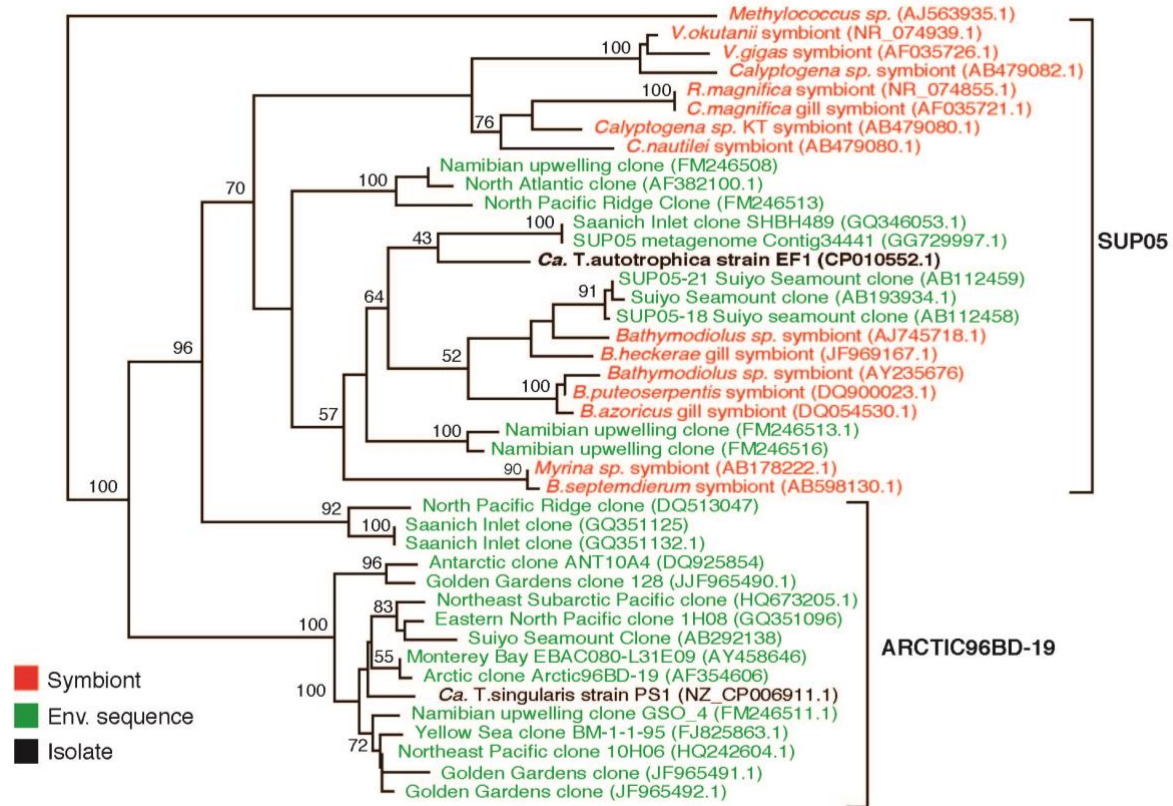


Figure 2.2. Chemoautotrophic growth of “*Ca. T. autotrophicus*” strain EF1 under aerobic and anaerobic growth conditions. (A) Aerobic growth on copiotrophic seawater media from Puget Sound amended with 1mM $S_2O_3^{2-}$. (B) Anaerobic growth on seawater media bubbled with either N_2 only or $N_2:CO_2$ gas mix and amended with 1mM $S_2O_3^{2-}$ and 100 $\mu M NO_3^-$. The controls were not amended with $S_2O_3^{2-}$, NO_3^- or CO_2 . Experimental treatments were conducted in triplicate.

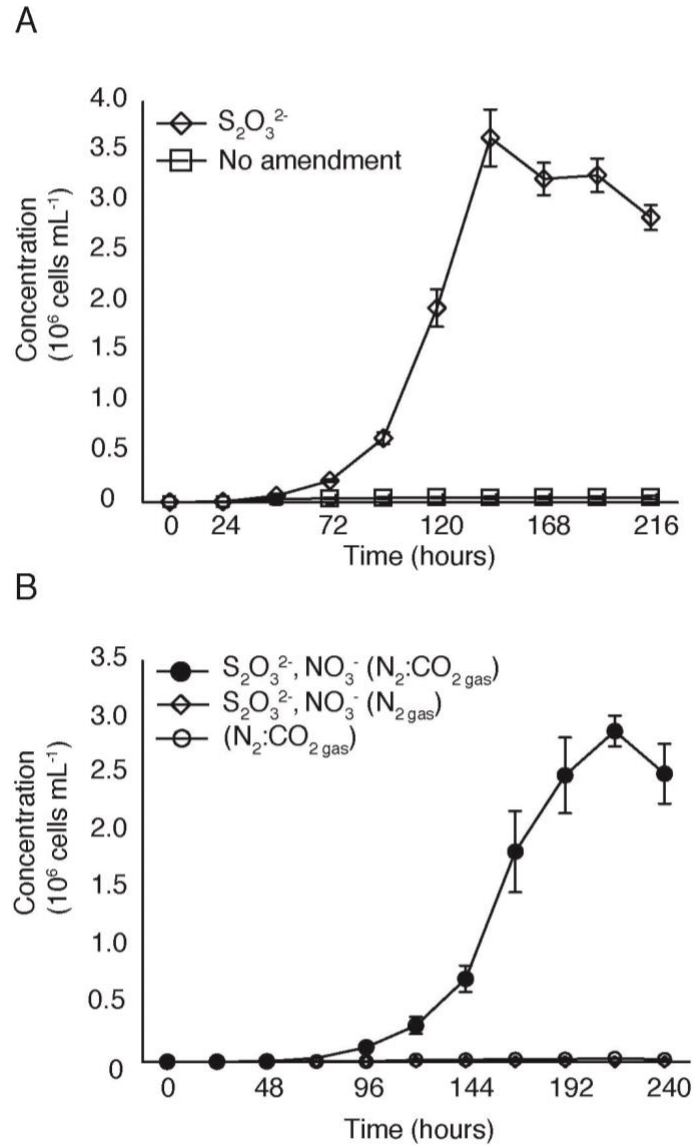


Figure 2.3. Nitrogen utilization by “*Ca. T. autotrophicus*” strain EF1 on copiotrophic media. (A) Anaerobic growth on seawater media from Puget Sound with *in situ* concentrations of NO_3^- (32 μM) and amended with 100 μM of additional NO_3^- (total = 132 μM). (B) Concentrations of NO_3^- , NO_2^- , and NH_4^+ . (C) Concentrations of only NH_4^+ . (D) Concentrations of N_2O measured by gas chromatography (Supplementary Materials and Methods). Experimental treatments were conducted in triplicate and nitrogen was measured at initial (T_0 hour) and final (T_{192} hour) time points.

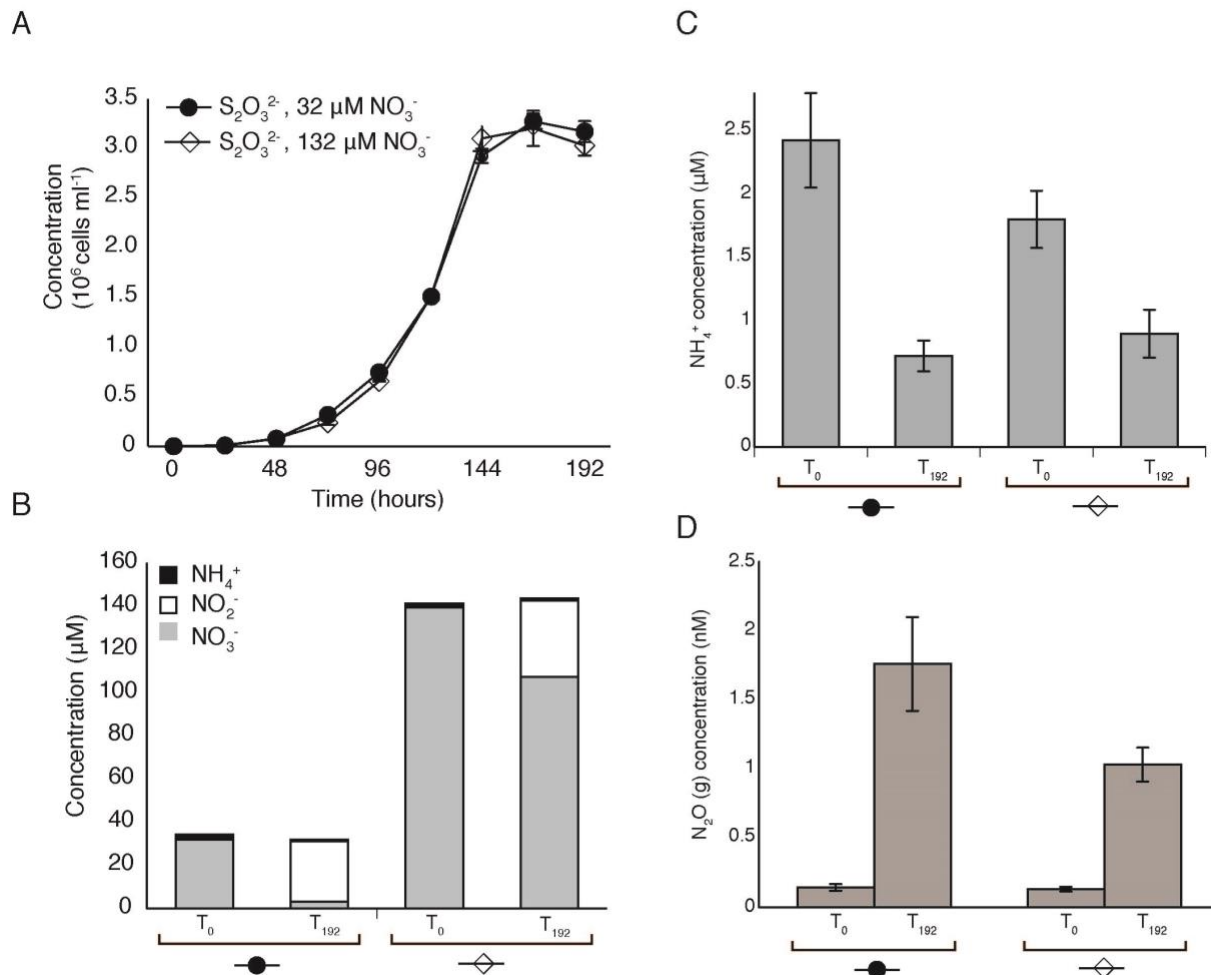


Figure 2.4. Nitrogen utilization of “*Ca. T. autotrophicus*” strain EF1 on oligotrophic media.

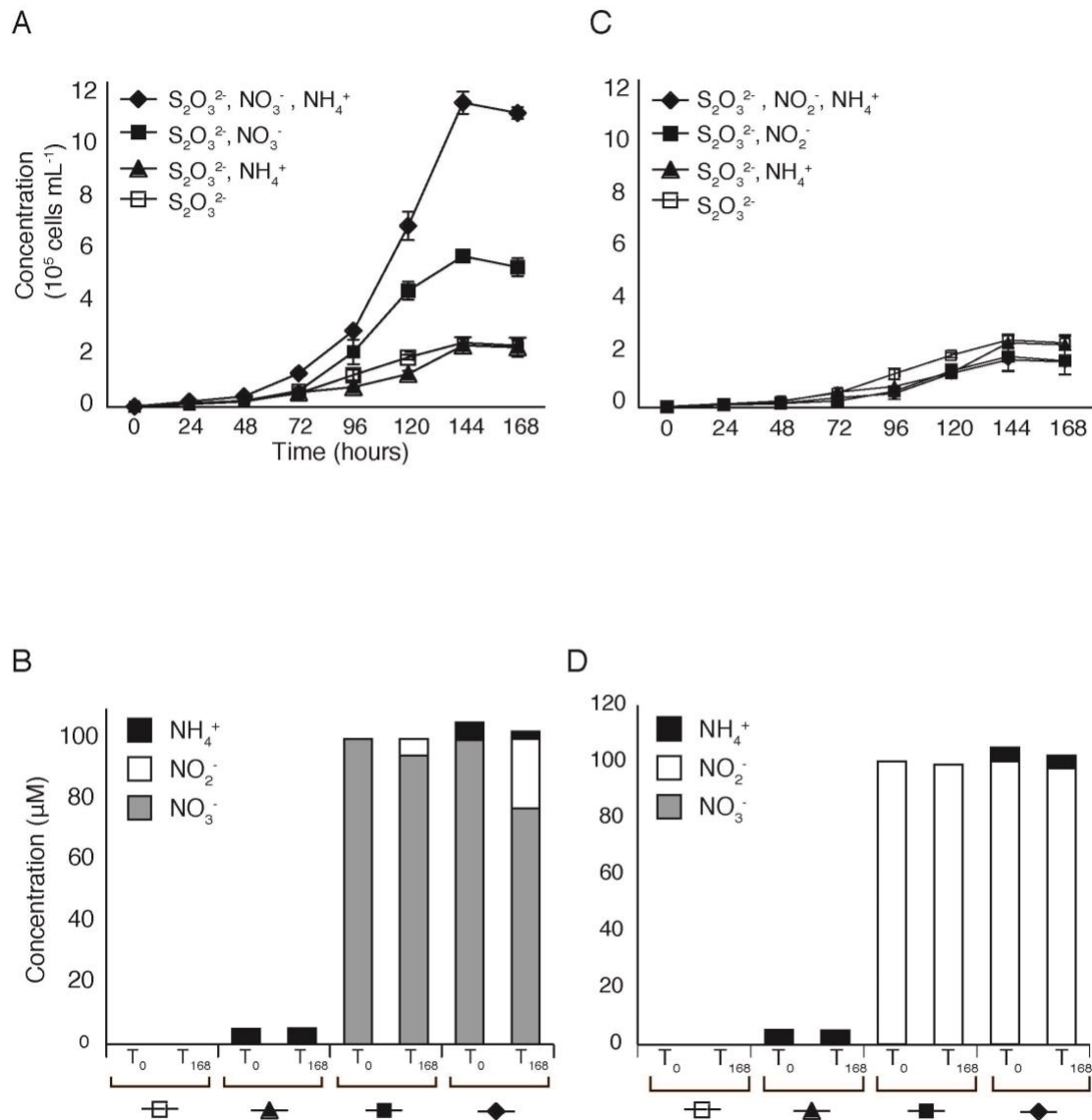
Anaerobic growth on seawater media from the Sargasso Sea amended with (A) NO_3^- (100 μM),

NH_4^+ (5 μM) and with only $\text{S}_2\text{O}_3^{2-}$ (1 mM) and (B) NO_2^- (100 μM), NH_4^+ (5 μM) and with only

$\text{S}_2\text{O}_3^{2-}$ (1 mM). (C and D) Concentrations of NO_3^- , NO_2^- and NH_4^+ measured at initial (T_0 hour) and

final (T_{168} hour) time points in (A) and (B), respectively. All experimental treatments and nutrient

measurements were conducted in triplicate.



2.7 ADDITIONAL INFORMATION

2.7.1 Fluorescence in situ hybridization (FISH).

SUP05 clade specific probe (GSO1032) and optimal hybridization conditions were obtained from a previously published study from the Mediterranean Sea that successfully enumerated this group of bacteria (Glaubitz et al., 2013). 10 ml of batch culture at a final cell density of 8×10^5 cells per ml was fixed with 10% formalin overnight and then filtered onto a 25 mm $0.2 \mu\text{m}$ white polycarbonate filter. Filters were subsequently hybridized overnight in hybridization buffer (900 mM NaCl, 20 mM Tris (pH 7.4), 0.01% (w/v) sodium dodecyl sulfate (SDS), 15% formamide), and then washed twice in hybridization wash (150 mM NaCl, 20 mM Tris (pH 7.4), 6 mM ethylenediaminetetraacetic acid (EDTA) and 0.01% SDS) for two 10 min intervals at 55°C . Nucleic acid staining occurred by mounting the filters with a DAPI/citiflour solution at a final concentration of $5 \mu\text{g ml}^{-1}$. Images were captured using a CoolSnap HQ CCD camera (Supplementary Figure 2).

2.7.2 Transmission Electron Microscopy

Cells were fixed overnight in 2% Paraformaldehyde/2% Glutaraldehyde (half strength Karnovsky's fixative) buffered with 0.2M Cacodylate buffer. Samples were dehydrated in an ethanol series (30%, 50%, 70%, 96 and 100%) for 20 minutes each, followed by two washes in propylene oxide for 15 minutes. Cells were negatively stained on a carbon-coated grid using 3% uranyl acid overnight and visualized under a JEOL JEM 1400 transmission electron microscope at the Fred Hutch Research Institute, Seattle, WA.

2.7.3 Dissolved nutrient measurements

NO_3^- and NO_2^- were reduced to NO in hot iodine solution followed by NO detection using a Teledyne 200E chemiluminescence NOx analyzer (Granger & Sigman, 2009). NH_4^+ was measured at the Seawater Analysis lab, University of California, Santa Barbara using a flow injection analyzer (Quikchem 8000, Lachat Instruments, Zellweger Analytics, Incorporated).

2.7.4 Gas measurements

100 μM of ^{15}N labeled KNO_3 (Sigma Aldrich) was used as a terminal electron acceptor for growth (Supplementary Figure 4C). N_2 concentrations were quantified in the headspace of triplicate no-growth controls and in treatments after cells reached early stationary growth phase ($\sim 10^6$ cells/ml). N_2 production was measured by transferring 6 ml of headspace into 12 ml He-purged exetainers (Labco Inc.). N_2 gas in exetainers was isolated by gas chromatography and mass ratios 29:28 and 30:28 were measured using a Finnigan Delta XL isotope ratio mass spectrometer. N_2 production rates were calculated following de Brabandere and colleagues (de Brabandere et al., 2013). N_2O was measured using gas chromatography and referenced to certified gas standards (0.1 M N_2O cylinder, Scott Specialty Gases). The final concentration of N_2O in bottles, dissolved as well as in the headspace, was calculated using a method previously described by Weiss & Price (Weiss & Price, 1980).

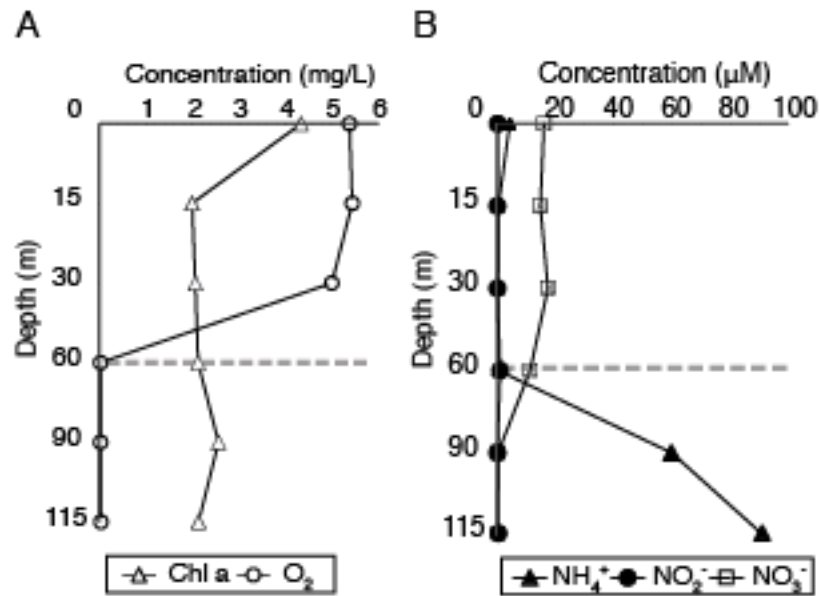
2.8 SUPPLEMENTARY REFERENCES

1. De Brabandere L, Canfield DE, Dalsgaard T, Friederich GE, Revsbech NP, Ulloa O, *et al.* (2013). Vertical partitioning of nitrogen-loss processes across the oxic-anoxic interface of an oceanic oxygen minimum zone. *Environ Microbiol* **16**:3041–54.
2. Granger J, Sigman DM. (2009). Removal of nitrite with sulfamic acid for nitrate N and O isotope analysis with the denitrifier method. *Rapid Commun Mass Spectrom* **23**:3753–3762.
3. Weiss RF, Price BA. (1980). Nitrous oxide solubility in water and seawater. *Mar Chem* **8**:347–359.

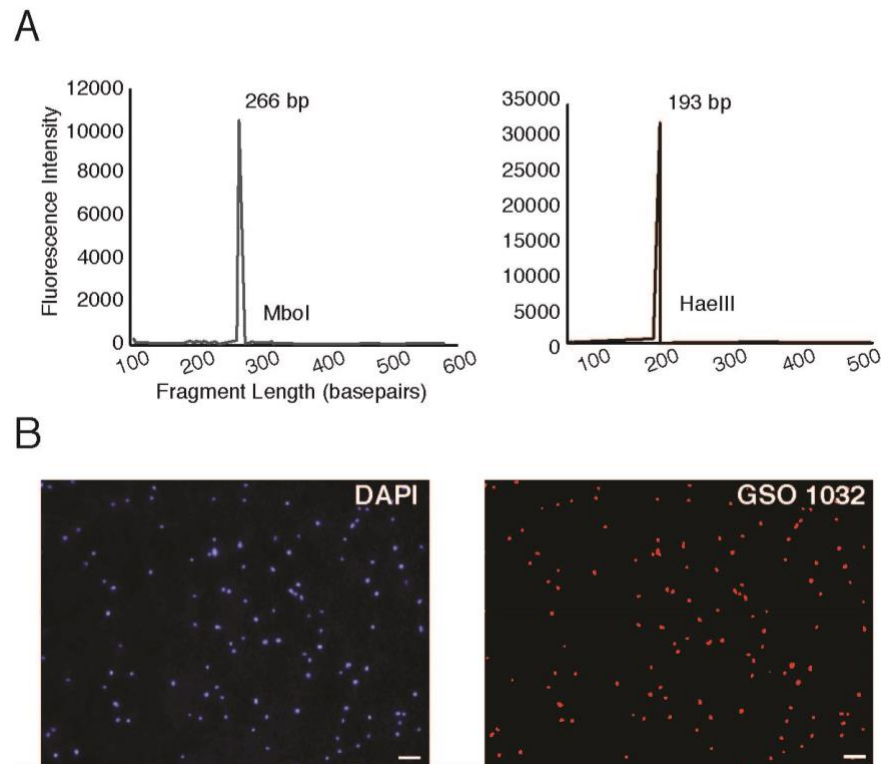
Supplementary Table 2.1. Nutrient concentrations in seawater used to make media. Media used for growth experiments included high nutrient (copiotrophic) and low nutrient (oligotrophic) seawater collected from Puget Sound and the Sargasso Sea, respectively. Nutrients and dissolved organic carbon (DOC) were measured after the media was filter sterilized.

| | Copiotrophic Seawater (Puget Sound, Oct 2014) Depth: 80m | Oligotrophic Seawater (BATS, March 2015) Depth: Surface |
|------------------------------|--|---|
| NO ₃ ⁻ | 32.20 μM | 0.15 μM |
| NO ₂ ⁻ | 0.023 μM | 0.02 μM |
| NH ₄ ⁺ | 2.22 μM | 0.04 μM |
| DOC | 107 μM | 72 μM |

Supplementary Figure 2.1. Nutrient profiles from Effingham Inlet. (A) Chl A and oxygen concentrations. (B) NH_4^+ , NO_3^- and NO_2^- concentrations. Gray dotted line indicates depth where water was collected for media and used to isolate “*Ca. T. autotrophicus*” strain EF1.

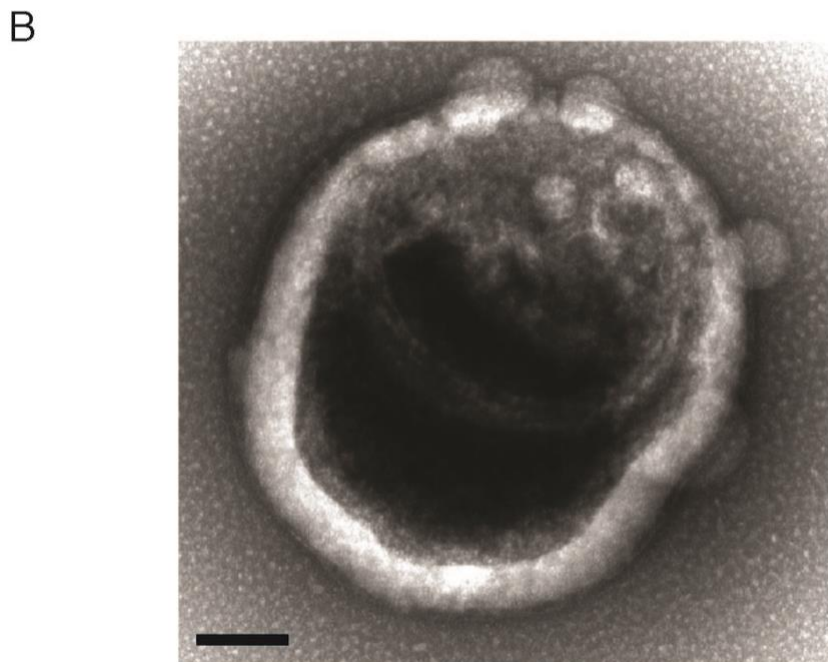
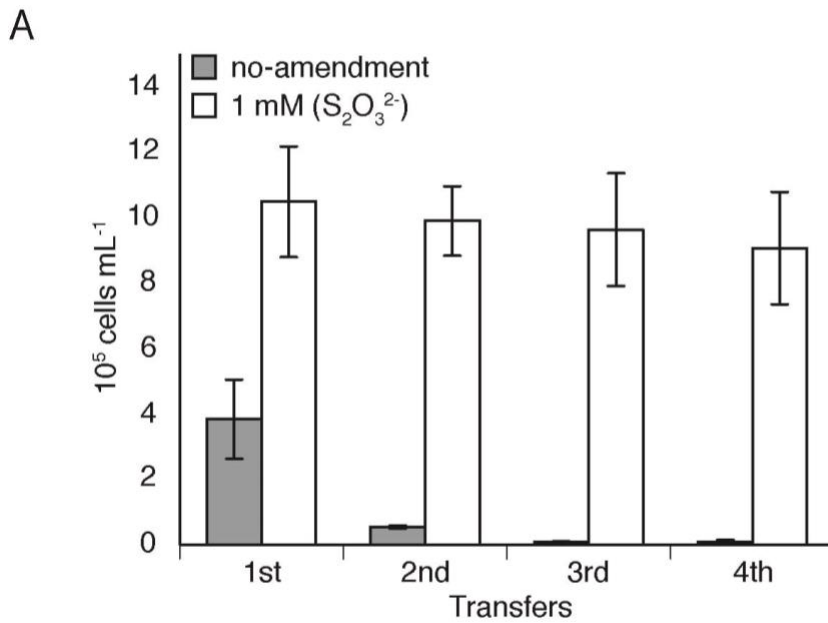


Supplementary Figure 2.2. Verification of “*Ca. T. autotrophicus*” strain EF1 purity. (A) Terminal restriction fragment length polymorphism (TRFLP) analysis with restriction enzymes MboI and HaeIII. Single peaks (266 bp and 193 bp) matched the predicted fragment lengths for SUP05. (B) Representative epifluorescence microscopy images of EF1 cells stained with the nucleic acid stain DAPI, and cells hybridized to the SUP05-specific FISH (fluorescence in situ hybridization) probe GSO-1032. Scale bar is 1 μ m.

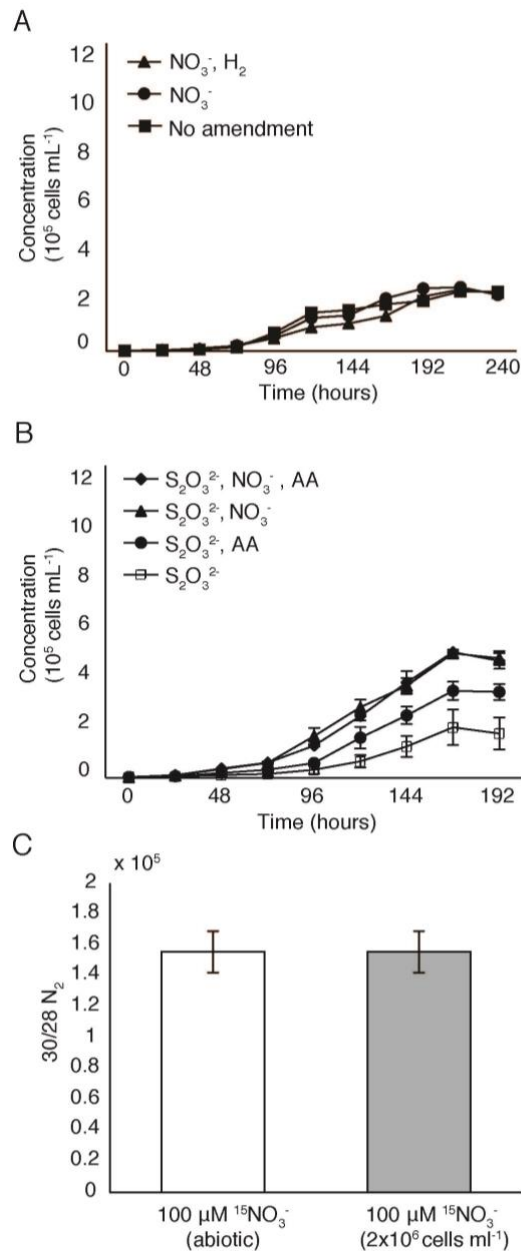


Supplementary Figure 2.3. Reduced sulfur requirement for “*Ca. T. autotrophicus*” strain EF1.

(A) Aerobic growth on seawater media with and without $S_2O_3^{2-}$ (1 mM) over four subsequent transfers. 1000 cells/ml were transferred to new media every five days. Experimental treatments were conducted in triplicate. (B) Negative strain transmission electron microscope image of “*Ca. T. autotrophicus*” strain EF1. Scale bar is 100 nm.



Supplementary Figure 2.4. Evaluation of electron donor (H_2), organic nitrogen source (amino acids), and product of denitrification (N_2). (A) Anaerobic growth on seawater media amended with H_2 gas (0.01 %) and NO_3^- (100 μM). (B) Anaerobic growth on oligotrophic seawater media amended with NO_3^- (100 μM) and an amino acid mixture (5 μM of N) $S_2O_3^{2-}$ (1 mM). (C) Measurement of ^{15}N labeled N_2 production. Experimental treatments and gas measurements were conducted in triplicate.



2.9 ACKNOWLEDGMENTS

I thank Dr. Richard Keil and captain and crew of *R/V Thomas G. Thompson* for their assistance during the senior thesis cruise of 2013. I am grateful to Brian Peters, Dr. Gordon Holtgrieve, Dr. Paul Quay, Dr. Dave Stahl, and Wei Qin for technological support in making nutrient and gas measurements. I thank Rachel Parsons and Bermuda Institute of Ocean Sciences for help collecting oligotrophic seawater media. This work was supported by grants from the National Science Foundation (OCE-1232840 and DGE-1068839).

Chapter 3. OXYGEN DRIVES DRAMATIC SHIFTS IN METABOLIC ACTIVITY OF CHEMOAUTOTROPHIC SUP05 ISOLATE, CANDIDATUS *THIOGLOBUS* *AUTOTROPHICUS*

Shah, V., Zhao, X., Nicastro, D., Ingalls, A., Morris RM. Sulfur uptake and storage in SUP05 extends the influence of the cryptic marine sulfur cycle to the oxygenated ocean (in prep)

3.1 ABSTRACT

Microbial metabolisms that yield energy from reduced sulfur are common in anoxic environments. Yet, the concentrations of many reduced sulfur species are below detection limits in seawater where sulfur bacteria thrive, such as oxygen-minimum zones (OMZs). This contradiction suggests a cryptic sulfur cycle in anoxic marine waters where rapid redox cycling of sulfur eludes detection but can result in significant carbon fixation. Using growth experiments, carbon measurements, EM images and protein expression I show that a facultative anaerobe from the SUP05 clade, “Ca T. autotrophicus”, grows at below-detection (<1 μM) of sulfur, stores sulfur in intracellular globules and exhibits enhanced sulfur storage and increased biomass under aerobic conditions. I show a metabolic shift in aerobic versus anaerobic cells using protein expression data. “Ca T. autotrophicus” cells display stark differences in expression of key carbon, nitrogen and sulfur metabolism genes in aerobic versus anaerobic environments. These observations support the cryptic sulfur cycle in anoxic marine waters and extend the influence of

sulfur cycling to chemosynthetic biomass production in the oxygenated ocean, and help to explain the success of a metabolically flexible group of organisms that cross oxic/anoxic boundaries.

3.2 INTRODUCTION

Marine microorganisms that use sulfur for energy yielding reactions are frequently identified at oxic-anoxic interfaces. In these reactions, sulfur compounds can serve the roll of electron acceptors (sulfate reduction) or electron donors (sulfur oxidation). Both these processes play an important role in oxygen depleted, nitrate-rich environments like oxygen minimum zones (OMZs), fjords, hydrothermal systems and enclosed seas (Ulloa et al 2012, Zaikova et al 2012, Wright et al 2012, Hawley et al 2014). Environmental studies indicate that members of the SUP05 clade of gamma-sulfur oxidizing (GSO) proteobacteria are abundant in various environments where they experience a range of sulfur compounds. The utilization of these sulfur compounds is limited by concentration and in part controlled by the oxygen gradient within these environments (Keeling 2009).

Anoxic waters in the eastern tropical north pacific (ETNP), eastern tropical south pacific (ETSP), Arabian Sea and South Atlantic experience episodic inputs of sulfide associated with upwelling near continental shelves (Hawley et al 2014, Glaubitz et al 2013). In contrast, anoxic waters in fjords and enclosed water bodies are less frequently ventilated and highly enriched in sulfide (Canfield et al 2010). SUP05 are particularly abundant in anoxic waters enriched in sulfide, but have also been identified in non-sulfidic OMZs where the concentrations of sulfide fall below detection limit (Glaubitz et al 2013). Evidence of active sulfur cycling was reported from the ETSP with no detectable sulfide, suggesting that a cryptic sulfur cycle links the marine carbon

and nitrogen cycles in both sulfidic and non-sulfidic oxygen depleted environments (Glaubitz et al 2013). Organic sulfur is available in large quantities throughout these oxygen-depleted environments (Williams et al 2012). They can occur in the form of S-containing amino acids like cysteine, methionine and taurine or as osmolytes, or byproducts produced by clams at mussels. In the surface ocean, phytoplankton can convert methionine to a highly stable and soluble organic compound called DMSP (dimethylsulfoniopropionate). The effect of these organic compounds on dissimilatory sulfur cycles is not well understood.

Past environmental studies on the genome of SUP05 bacteria show that this group of organisms is metabolically versatile with the ability to use a wide variety of energy sources (Rogge et al 2017). Genomic data shows that SUP05 have the potential to store sulfur in the form of vesicular globules (Stewart et al 2015). These findings are further supported by data that show a representative isolate “Ca. T. autotrophicus”, that can use different electron acceptors (nitrate when anaerobic and oxygen when aerobic) and multiply up to two generations using stored reservoirs of sulfur (Stewart et al 2015). These findings indicate that the cryptic marine sulfur cycle extends across oxic/anoxic interfaces in diverse marine ecosystems and growth under different conditions can directly affect biomass production via SUP05 cells. In this study, I grew “Ca. T. autotrophicus”, under aerobic and anaerobic conditions in natural seawater media amended with different sources and concentrations of reduced organic and inorganic sulfur to test the cryptic sulfur cycle hypothesis and elucidate its effects on chemoautotrophic biomass production across the oxic-anoxic transition.

3.3 MATERIALS AND METHODS

3.3.1 *Aerobic and anaerobic growth conditions*

“*Ca. T. autotrophicus*” cells were grown as previously described (Marshall & Morris 2012, Shah et al 2017), with modifications. Media was prepared by filter sterilizing seawater collected from Puget Sound using a tangential flow filtration system equipped with a 30kDa filter (Millipore, NJ USA). Media was stored, and checked for cells to ensure it was contaminant free and subsequently distributed into acid washed and autoclaved 125 mL glass serum bottles. Aerobic media bottles were covered with sterilized aluminum foil. Anaerobic media bottles were sealed with 20 mm butyl rubber stoppers (Wheaton, Millville, NJ USA), then bubbled with an N₂:CO₂ gas mix that contained 1000 ppm CO₂, (Praxair, Danbury CT USA) for 10 minutes, then headspace sparged for an additional 5 minutes. Oxygen removal was verified by adding BD GasPak™ anaerobic strips (BD, Franklin Lakes, NJ USA) to un-inoculated serum bottles. Batch cultures used for cryo-tomography and CHN analysis were amended with additional 5 μM of NH₄⁺ and 30 μM of NO₃⁻ to ensure highest cell yields as previously described (Shah et al 2017).

3.3.2 *Sulfur growth and sulfur deplete conditions*

Sulfur-depleted cells were required to evaluate growth with alternative electron donors. This was achieved by successively transferring cells into natural un-amended seawater media, as previously described (Shah et al 2017). Briefly, cells from cultures in exponential growth phase were transferred from natural seawater media amended with 1 mM thiosulfate to un-amended seawater media (T1). Cultures were incubated for four days, at which time cells were transferred to fresh un-amended seawater media (T2) and incubated for four days. Cells from T2 were

deemed sulfur-deplete. This was verified under aerobic and anaerobic growth conditions by conducting a sulfur-depletion experiment in triplicate, and by adding a third transfer (T3). No growth was detected in the final transfer. All incubations were at 13°C. Growth on different sulfur compounds was determined under aerobic and anaerobic growth conditions by adding sulfur-deplete cells to serum bottles containing 10 µM of reduced sulfur (thiosulfate, sulfide, polysulfide, cysteine, methionine, taurine, thiotaurine, hypotaurine, or DMSP) (Fisher BioReagents, WA USA, Wako Chemicals, USA). DMSP was obtained from the Moran research group (University of Georgia, USA) (Reisch et al 2011). Growth with different concentrations of reduced sulfur was determined under aerobic and anaerobic growth conditions by adding sulfur-deplete cells to serum bottles containing 0.01, 0.1, 1.0, 10 or 100 µM of reduced sulfur (thiosulfate, sulfide, thiotaurine). Only anaerobic conditions were tested for sulfide, since it rapidly oxidizes in the presence of oxygen (Pruski & Fiala-Médioni 2003). All growth experiments were conducted in biological triplicates incubated at 13°C and started with the same initial cell concentration (1×10^3 cells/mL).

3.3.3 *Cryo-electron Tomography*

Frozen-hydrated specimens were prepared as described previously (Zhao et al 2017). Briefly, *T. autotrophicus* strain “Ca. *T. autotrophicus*” cells were harvested by centrifuging at 39,000-x g at 4°C for 1 hour and then re suspended in 100 µL seawater media. Quantifoil grids (Copper, R2/2) with holey carbon film and lacey carbon grids were positively glow discharged for 30s at 30 mA. 3 µL volumes of cell solution were added onto the grid, and then the cells were mixed with 1 µL of 10-fold concentrated solution of 10-nm BSA colloidal gold (Sigma-Aldrich, St. Louis, MO) (Iancu et al 2007). Excess fluid was blotted from the backside of grid with Whatman filter paper

for ~2 seconds. Then, the grid was plunge frozen in liquid ethane at -170 °C using a homemade plunge freezer. Cells were imaged using Titan Krios 300 kV FEG transmission electron microscope (FEI Company, Hillsboro, OR) equipped with a post-column Gatan imaging filter (Gatan, Pleasanton CA) and Volta Phase Plate (FEI). Images were recorded at 26, 000 magnification using a K2 Summit direct electron detector (Gatan, Pleasanton CA) with an effective pixel size of 5.5 Å. Tilt series were acquired using Serial EM software (Mastrorarde et al 2005, Johnston et al 2007) under low-dose mode and were recorded from -60° to +60° in 2° increments, with a cumulative dose of ~100 e-/Å. The defocus was set to 0 µm when using phase plate and the energy filter was in zero-loss mode with a slit width of 20eV. The tilt series images were aligned by the IMOD software package) using the 10 nm gold nanoparticles as fiducial markers. The tomographic reconstructions were calculated by weighted back projection using IMOD software package.

3.3.4 *Carbon, Hydrogen and Nitrogen Measurements*

Aerobic and anaerobic cultures of “*Ca. T. autotrophicus*” were filtered at highest cell yield (early stationary phase) on 25mm (baked at 450°C for 4.5 hrs.) GFS75 glass fiber filters (Fisher Scientific, NJ USA). Due to variable pore sizes of glass fiber filters, loss of cells during filtration was quantified by measuring cell concentration of media pre and post-filtration. Filtration of aerobic media resulted in a total of 6.50×10^9 cells collected on filter (4.5% lost in filtrate) whereas filtration of anaerobic media resulted in 1.46×10^{10} cells collected on filter (11% lost in filtrate). Un-inoculated media was also filtered, as a control sample, to account for background carbon, hydrogen and nitrogen contamination. Filters were stored inside aluminum foil (baked at 450°C for 4.5 hrs.) and frozen at -80°C. Carbon, hydrogen and nitrogen content in filters were

analyzed using an Exeter CE-440 CHN Auto Analyzer. Final values of carbon, nitrogen and hydrogen per cell were adjusted using control values (less than 0.05%).

3.3.5 Proteomics: Cell Growth and Collection

“*Ca. T. autotrophicus*” cells were grown at in situ temperatures (13 °C) in acid-washed and autoclaved 125 ml serum vials containing seawater media from Puget Sound. Media was made using seawater was collected from Puget Sound on April 20th, 2017 and analyzed for nutrients (28 μM of NO₃⁻, 4.8 μM of NH₄⁺ and 98 μM C per liter of dissolved organic carbon). Two sets of “*Ca. T. autotrophicus*” cultures were grown under either aerobic or anaerobic conditions. Aerobic cultures were maintained in 10 serum bottles containing 100 ml of seawater media each and amended with 1 mM sodium thiosulfate. Anaerobic cultures were maintained in 10 serum bottles contained 100 ml of seawater amended with 1 mM sodium thiosulfate, sealed with 20 mm butyl rubber stoppers (Wheaton), then bubbled with an N₂:CO₂ gas mix (1000 ppm CO₂, Praxair Specialty Gas Mix) for 10 minutes, and headspace sparged for an additional 5 minutes. Complete removal of oxygen inside serum bottles was confirmed using BD GasPak anaerobic strip added to an un-inoculated control serum bottle. A media blank was also prepared to serve as a control. Cell biomasses from the cultures were filtered when they reached early stationary growth phase (~5 × 10⁶ cells per mL). Cell biomass from aerobic cultures of “*Ca. T. autotrophicus*” (total of 1 L) was filtered onto a single Durapore filter (0.22 μm, 47 mM), corresponding to a total of 4.55 × 10⁹ cells. Cell biomass from anaerobic cultures (total of 1 L) was filtered onto a single Durapore filter, where filtering was done inside an anaerobic glove bag containing N₂ gas to avoid exposure of cells to oxygen, corresponding to 4.90 × 10⁹ cells. A media blank was also collected onto a single filter. All filters were stored at -80 °C until extraction.

3.3.6 *Proteomics: Protein Extraction and In-solution Proteolytic Digestion*

Filters from “Ca. T. autotrophicus” (aerobic) and “Ca. T. autotrophicus” (anaerobic) were thawed from -80 °C, cut using sterile scissors and each filter was cut in half and re-suspended in 0.5 mL of 50 mM ammonium bicarbonate (AMBIC) with 5 mM ethylenediaminetetraacetic acid disodium salt dihydrate (EDTA) buffer (pH 8) in a microcentrifuge tube containing glass beads. Control filters containing only the media blank were processed alongside as well as sample tubes containing only the AMBIC/EDTA buffer served as sample processing controls. Each filter suspension was subjected to bead beating for 30 seconds at 6 m/s, frozen at -20 °C for 45 minutes, and thawed. The bead-beating and freeze-thaw cycles were repeated twice followed by a third bead-beating cycle and an overnight freeze at -20 °C. Frozen filter re-suspensions were thawed, cells further disrupted by vortexing with beads, and then centrifuged at 7,000 rpm (4,602 rcf) for 2 minutes. A 250 µL aliquot from each tube containing the one-half of its corresponding filter was combined into a new 2 mL protein LoBind eppendorf tube for proteomic processing (see below), resulting in a total of 500 µL of protein extract for each of the “Ca.T.autotrophicus”(aerobic) and “Ca.T.autotrophicus” (anaerobic) samples.

Estimated bulk protein concentration for lysed cell extracts were measured using the Lowry assay (DC protein assay, Bio-Rad). Lowry assay samples were prepared following the manufacturer protocol adapted for analysis using a microcuvette (requiring only 5 µL of sample). Protein concentrations were analyzed using a spectrophotometer (BeckmanCoulter DU800) and determined by comparing sample absorbance units to a bovine serum albumin (BSA) protein concentration calibration curve (prepared only in 50 mM AMBIC, 5 mM EDTA). For downstream proteomics analyses, I also calculated approximate protein concentration from cell

density measurements where I assume an 80% extraction efficiency to lyse cells by bead beating. Thus, I have estimated 1.82×10^9 cells (~18 μg) and 1.96×10^9 cells (~19 μg) for “Ca.T.autotrophicus” (aerobic) and “Ca.T.autotrophicus” (anaerobic), respectively, were used for downstream proteomics analyses. Lysed cells (500 μL) were subjected to in-solution proteolytic digestion. First, RapiGest SF (Waters), an acid labile surfactant, was added to help facilitate protein solubilization (0.06% w/v). Next, disulfide bonds were reduced with tris(2-carboxyethyl) phosphine (TCEP; to a final concentration of 10 mM) for 1 hr at room temperature in the dark. Reduced samples were then alkylated with iodoacetamide (IAM; to a final concentration of 30 mM) for 1 hour at room temperature in the dark. Excess IAM was quenched by the addition of dithiothreitol (DTT; to final concentration of 5 mM) for 1 hr at room temperature in the dark. All protein extracts were proteolytically digested with mass spectrometry-grade trypsin/Lys-C mix (Promega) at an estimated substrate-to-enzyme ratio of 25 for 19 hours at 37 °C containing a final concentration of 0.05% w/v RapiGest, 50 mM AMBIC and 5 mM EDTA (pH 8). Following trypsin/Lys-C digestion, RapiGest was hydrolyzed by the addition of trifluoroacetic acid (0.5% final v/v, pH < 2; concurrently terminating trypsin/Lys-C activity), heated for 45 minutes at 37 °C and centrifuged at 15,000 rpm (21,130 rcf) at 4 °C for 15 minutes to precipitate the water immiscible decomposition product, dodeca-2-one. The supernatant was removed, transferred to a new protein LoBind eppendorf tube and samples were dried to near-dryness using a centrivap concentrator (Thermo Savant SPD2010 SpeedVac). Digested samples were desalted using a MacroSpin C18 column (NestGroup) following an established manufacturer protocol. Samples were eluted from the MacroSpin columns using two times 200 μL of 80% LCMS-grade acetonitrile with 20% LCMS-grade water containing 0.1% LCMS-grade formic acid. Desalted samples were concentrated using the centrivap to near dryness and were

immediately resuspended in 95% LCMS-grade water with 5% LCMS-grade acetonitrile containing 0.1% LCMS-grade formic acid. The resuspension solution also contained an internal standard of synthetic peptides (Hi3 Escherichia coli Standard, Waters) at 50 fmol/ μL . All samples including controls were resuspended in 25 μL , corresponding to an estimated 7.29×10^7 cell/ μL for “Ca.T. autotrophicus” (aerobic) and 7.84×10^7 cells/ μL for “Ca.T. autotrophicus” (anaerobic). Samples were immediately analyzed by LCMS. Samples were injected in triplicates onto the column of a Waters ACQUITY M-class UPLC; an injection volume of 2 μL corresponded to an on-column estimated 1.46×10^8 cells (1.45 μg) for “Ca.T. autotrophicus” (aerobic) and 1.57×10^8 cells (1.56 μg) for “Ca.T. autotrophicus” (anaerobic). Peptide separation was performed by reversed-phase chromatography using a nano ACQUITY HSS T3 C18 column (1.8 μm , 75 μm x 250 mm; 45 °C) with an ACQUITY UPLC M-class Symmetry C18 trapping column (180 μm x 20 mm). The peptides were trapped at a flow rate of 5 $\mu\text{L}/\text{min}$ at 99% A for 3 minutes. A flow rate of 0.3 $\mu\text{L}/\text{min}$ was used over a gradient between LCMS-grade water (A) and LCMS-grade acetonitrile (B), both modified with 0.1% LCMS-grade formic acid. The total 145-minute gradient method for the separation of the peptides started at 95% A and ramped to 60% A over the course of 120 minutes. The gradient then switched to 15% A at 122 -127 minutes followed by a ramp back to starting conditions 95% A at 128-145 minutes. The ACQUITY M-class was coupled to a Thermo QExactive HF Orbitrap high-resolution mass spectrometer (HRMS) equipped with a nano-electrospray (NSI) source made in-house following the University of Washington Proteomic Resource (UWPR) design. Using a MicroTee (PEEK, 0.025” OD), the commercial analytical column was connected to a commercial emitter (PicoTip, Waters) and the liquid path was applied a high voltage through a platinum wire (adapted from UWPR design). All analyses were carried out in positive mode and a NSI spray voltage of 2.0

kV. Data was collected using data dependent acquisition (DDA) using Xcalibur 4.0 data acquisition software (Thermo Fisher). The MS¹ scan range was 400-2000 *m/z* at 60,000 resolutions with a maximum injection time of 30 ms and automated gain control of 1e6. Following each MS¹ scan, data-dependent MS² (dd-MS²) was set to perform on the top 10 ions in a data-dependent manner at 15,000 resolutions with normalized collision energy of 27 eV. Additional selection criteria for dd-MS² were as follows: maximum injection time of 50 ms with an automated gain control of 5e4, the isolation window was 1.5 Da and dynamic exclusion was set at 20 sec.

3.3.7 *Data Analysis and Protein Identification*

Data processing was conducted using the software from the trans-proteomic pipeline (TPP v.4.8.1).¹ Briefly, raw data was converted to mzML and searched using COMET^{2,3} against a FASTA protein database consisting of “Ca.T.autotrophicus” (Uniprot 9GAMM 1,488 proteins accessed February 2017; KEGG estimated protein genes 1,506), the *E.coli* chaperone protein (Hi3 standard; P63284), and was concatenated with a set of randomized sequences. Additional COMET parameters included trypsin enzyme specificity; one allowed non-tryptic termini, up to two missed cleavage sites, carbamidomethylation of cysteine residues as a fixed modification (+57.02146 Da), and oxidation of methionine residues (+15.9949 Da) and clipping of N-terminal methionines as variable modifications. The COMET pep.xml files from each technical triplicate mzML file were searched in PeptideProphet with greater than 90% peptide probability followed by iProphet⁴ and ProteinProphet⁵ within the TPP. The COMET pep.xml files from each technical triplicate mzML file were also grouped and searched using the same parameters in PeptideProphet and iProphet. The set of randomized sequences were decoy peptides used for the

purpose of calculating peptide spectrum matching (PSM) and protein false discovery rates (FDR). From each of the combined datasets, PeptideProphet probabilities greater than 90% resulted in the following *T.autotrophicus* (aerobic or anaerobic). *T.autotrophicus* aerobic resulted in 5,276 peptides and 66,326 PSM with a corresponding FDR of <0.05% (PSM level 28/66,326). *T.autotrophicus* anaerobic resulted in 5,019 peptides and 52,070 PSM with a corresponding FDR of <0.1% (PSM level 38/52,070). The list of protein identifications was filtered using a 95% or greater protein probability as calculated from iProphet corresponding to a FDR < 0.5%; where 884 total proteins identified across both treatments, representing approximately 59% of all the predicted proteins encoded in the “Ca. T. autotrophicus” genome. Under aerobic conditions, 793 (53%) “Ca.T.autotrophicus” proteins were identified and under anaerobic conditions, 740 (49%) “Ca.T.autotrophicus” proteins were identified.

3.3.8 *Label-free comparison of relative protein abundances across “Ca.T.autotrophicus” growth treatments*

To ensure adequate comparison of relative protein abundances across “Ca. T. autotrophicus” treatment conditions, I further filtered the protein datasets where at least one peptide (or spectral counts) must be observed consistently across individual injections and the protein probability within each replicate must be greater than 95%. Data filtering based on these constraints was done using output from Abacus.⁶ Abacus was used to join and organize PeptideProphet and ProteinProphet data across replicates and treatment conditions. In addition, Abacus calculates an adjusted spectral count using a weighted adjustment factor. Adjusted spectral counts are useful for appropriate assignment of spectral counts to proteins that have a high degree of sequence homology to each other and thus, a high number of shared peptides. For proteins without high

sequence homology, adjusted spectral counts are identical to total spectral counts, which are not weighted. Finally, all filtered Abacus datasets were further constrained by iProphet protein lists, which have validated protein probabilities greater than 95%, for each treatment. Following these data constraints, 802 total “Ca. T. autotrophicus” proteins were observed and used for comparative analyses representing 53% of all the predicted proteins encoded in the “Ca. T. autotrophicus” genome. This corresponded to 721 (48%) and 667 (44%) proteins under aerobic and anaerobic conditions, respectively (Figure S1). Media blank control sample analyzed alongside detected 29 proteins above 95% protein probability, including the Hi3 internal standard.

For each treatment, all total spectral counts as well as adjusted spectral counts were averaged across triplicate injections and standard deviations of these averages were calculated for error. It is worth noting that many of the proteins detected in the media blank control sample (29 proteins) had very high standard deviations, indicative of their presence as injection contaminants that decreased in abundance over triplicate injections. Averaged spectral counts of proteins were further normalized to the Hi3 internal standard to account for differences in NSI ionization of peptides due to sample matrix effects (Figure S5). To compare normalized spectral counts across “Ca.T.autotrophicus” treatment conditions and account for differences in biomass injected on-column, the relative amount of protein ‘per cell’ was calculated by dividing by the number of cells injected on-column (see above estimates), resulting in a semi-quantitative estimate of ‘normalized spectral counts per cell’ (with propagated error). The subcellular localization of each protein is based on predictions from PSORTb (v3.0). COG functional

categories and protein descriptions were generated using eggNOG-mapper and filtered using e-value scores less than $1e-40$.⁸

3.4 RESULTS

In a growth experiment two separate batches of “*Ca. Thioglobus autotrophicus*”, aerobic and anaerobic (Fig 1) at early stationary phase were used as inoculum. Cells from inoculum underwent successive transfers of 1000 cells into sulfur-deplete media (aerobic and anaerobic). I observed significant cell yield in both aerobic and anaerobic treatments despite multiple transfers into media with no reduced sulfur source. However, aerobic cells persisted longer whereas anaerobic cells yielded a higher final cell count. Under aerobic conditions, cells densities increased by more than an order of magnitude after the first two transfers into sulfur-deplete media and 2-fold after the third transfer, reaching 1.34×10^5 , 2.75×10^4 and 2.28×10^3 cells/ml, respectively. Cell densities increased by two orders of magnitude under anaerobic growth conditions after the first transfer into sulfur-deplete media and 3-fold following the second transfer, reaching 4.51×10^5 and 7.10×10^3 cells/ml, respectively. No significant growth was detected in the third transfer.

The carbon, hydrogen and nitrogen content of “*Ca. T. autotrophicus*” cells increased dramatically under aerobic growth conditions (Table 1). Cells contained approximately 3 times more carbon, 4 times more nitrogen and 10 times more hydrogen, in aerobic treatment. Cells grown to early stationary phase were visualized using cryo-electron tomography. Electron micrographs showed that “*Ca. T. autotrophicus*” cells were larger in volume and stored more sulfur under aerobic versus anaerobic growth conditions (Fig. 2). The average volume of cells grown in sulfur-replete media was approximately 3.9 times larger under aerobic conditions (Fig.

2A, B). Difference in the average volume of sulfur globules was even greater under aerobic versus anaerobic growth conditions (14-fold increase) (Table 2). Images further showed that “*Ca. Thioglobus autotrophicus*” cells were smaller and stored little to no sulfur under sulfur-deplete growth conditions (Fig. 2B and D). The average volume of cells grown in sulfur-deplete media was 3.79 and 1.11 times smaller than in sulfur-replete media under aerobic and anaerobic growth conditions, respectively (Table 2).

I tested the growth of “*Ca. Thioglobus autotrophicus*” cultures on nine different reduced sulfur sources (organic and inorganic) under aerobic and anaerobic conditions (Sup. Fig). Sulfide and Polysulfide were only tested under anaerobic conditions since these compounds oxidize abiotically in the presence of oxygen, thus rendering it challenging to distinguish between biotic versus abiotic oxidation of sulfur. Cells showed significant growth in two inorganic sulfur compounds (thiosulfate and sulfide) and one organic sulfur compound (thiotaurine) but were unable to use other sources of sulfur that are likely present in the diverse environments that SUP05 inhabit (i.e.: polysulfide, cysteine, methionine, taurine, hypotaurine and DMSP (3-(dimethylsulfaniumyl) propanoate)). Following this “*Ca. T. autotrophicus*” cells were tested under aerobic and anaerobic conditions across a range of concentrations (0.01-10 μM) of thiosulfate, sulfide and thiotaurine (Fig. 3). These included concentrations that fell well below detection limits of instruments used in field studies ($\sim 1 \mu\text{M}$) (Aumonda et al 2012). The highest specific growth rates were obtained under anaerobic conditions where sulfide (1 μM) was the electron donor and nitrate was the electron acceptor. Specific growth rate and doubling time of aerobic treatments were higher compared to anaerobic treatments thiosulfate and thiotaurine (Table 2). Using our cell specific growth rates and measurements of cell carbon content (Table

1), I calculate that “*Ca. Thioglobus autotrophicus*” cells fix between 0.70-1.66 fmoles of carbon/liter/day in anoxic waters and up to 4.38 fmoles of carbon/liter/day in oxic waters (Table 2).

Protein expressions of key metabolic genes were measured in “*Ca. Thioglobus autotrophicus*” cells grown under aerobic and anaerobic environments (Fig. 4). Both treatments were grown using thiosulfate as an energy source. Thiosulfate serves the role of a stable electron donor in both aerobic and anaerobic environments plus results in highest final cell yield (necessary for proteomic analysis). Data shows that in both treatments cells express the maximum number of proteins for production of an S-layer membrane and chemosynthetic metabolism, which broadly includes carbon (CO₂ fixation), sulfur (dissimilatory oxidation) and nitrogen (dissimilatory reduction) processing systems. (Fig. 4). I observed distinct differences in expression of carbon metabolism genes across aerobic versus anaerobic treatments. Aerobic cells expressed a greater ratio of RuBISCo form I genes versus RuBISCo form II, whereas the opposite was true for anaerobic cells where there was a greater ratio of RuBISCo form II versus form I. Nitrate reductase proteins (napHKZ) were upregulated in anaerobic treatment but completely absent in aerobic treatments. Whereas the gene NapA was upregulated in aerobic versus anaerobic treatment. The entire suite of sulfur oxidation genes including soxABXYZ, dsrABCH, dsbAD, thioredoxin (trx), and rhodanese sulfurtransferase (rhod-like) were expressed in both treatments. All aforementioned genes were unregulated in aerobic treatment except for dsbAD and dsrAB. Both treatments expressed the set of genes responsible for an incomplete TCA cycle. The TCA cycle genes were largely upregulated in the aerobic treatment. Both treatments expressed a large amount of membrane proteins, which includes S-layer protein (that constitutes 86% of the entire

proteome) and SGP protein that is responsible for the outer membrane of sulfur containing globules.

3.5 DISCUSSION

In the environment, SUP05 cells have been found in large, non-sulfidic OMZs where there is no detectable sulfide present (Canfield et al 2010, Wright et al 2012, Ulloa et al 2012). As strict chemoautotrophic sulfur oxidizers, SUP05 bacteria require a source of reduced sulfur in order to fix carbon and multiply (Walsh et al 2009, Zaikova et al 2010). Current literature describes this phenomenon within the cryptic sulfur cycle (Canfield et al 2010). The products of biogenic sulfate reduction (sulfide, thiosulfate and other reduced sulfur compounds) are rapidly oxidized by SUP05 bacteria, thereby rendering these chemical species undetectable (Rogge et al 2017). Alternatively, these bacteria may be using below detection limit sulfur or other sources of sulfur that were previously not considered a significant source of energy, i.e. organic sulfur (Ksionzek et al 2016). In this study, I use growth experiments to show that “*Ca. Thioglobus autotrophicus*” can continue to multiply over several generations in sulfur deplete media (Fig 1). But the growth of *T. autotrophicus* varies depending on availability of oxygen. In the presence of oxygen (used as terminal electron acceptor), cells continue to reach in situ cell densities over three subsequent transfers, whereas they only multiple for two in aerobic treatments. These data provide evidence that cells have some mechanism for sulfur storage that they can utilize during periods of energy starvation and that ability to store larger quantities of energy is oxygen dependent.

Cryo-electron tomography images showed that “*Ca. T. autotrophicus*” cells were larger and stored sulfur in multiple intracellular globules under aerobic versus anaerobic growth conditions (Fig 2A and D). Globules were determined to be modes of sulfur storage because cells lost their

globules after a period of growth in sulfur deplete conditions (Fig 2B and C). Aerobic cells were not only larger in volume (3.9 times), they had multiple globules (3-4 more) and the sulfur containing globules themselves were larger in volume (16 times). (Table 2). This increase in cell volume was accompanied with higher CHN content per cell in aerobic versus anaerobic treatment (Table 1). Aerobic cells general contained more biomass (3 times more C, 4 times more N and 10 times more H). These data suggest that cells use oxygen to not only store more sulfur but also more biomass. In the environment, SUP05 cells found at the oxic/anoxic interface may be responsible for a much larger portion contribution to the organic carbon pool. Using growth rates and CHN analyses, I estimate that in anaerobic environments SUP05 cells can fix approximately 0.70 to 1.66 fM C/cell/day whereas aerobic SUP05 can fix 3.25 to 7.49 fM C/cell/day (Table 2). The availability of oxygen as a terminal electron acceptor can allow SUP05 bacteria to fix 3-5 times as much carbon as anaerobic SUP05.

“Ca. Thioglobus autotrophicus” cultures reached in situ cell densities using inorganic and organic sources of reduced sulfur for energy (sulfide, thiosulfate and thiotaurine). Growth on inorganic sources of reduced sulfur is fairly common in marine environments, but evidence for use of an organic source, thiotaurine, is rare and has only been observed in symbionts in the past (Pruski et al 2000). In addition growth on all sulfur sources included concentrations that fell well below detection limits of instruments used in field studies ($\sim 1 \mu\text{M}$) (15). The highest specific growth rates were obtained under anaerobic conditions where sulfide ($1 \mu\text{M}$) was the electron donor and nitrate was the electron acceptor. The ability of “Ca. Thioglobus autotrophicus” to grow on sulfide at this low concentration implies that the half saturation constant for the flavocytochrome c sulfide dehydrogenase (fccAB) or the sulfide quinone oxidoreductase (sqr)

enzyme is in the sub-micromolar range. SUP05 are important players within the cryptic marine sulfur cycle that is intimately linked to nitrogen cycling in OMZs with no detectable sulfide (Canfield et al 2010, Rogge et al 2017). Our data showing that cultured SUP05 “Ca. T. autotrophicus” use stored, dilute and low concentrations of organic and inorganic sulfur across the oxic/anoxic transition provides a mechanism for SUP05 to remain actively growing under sulfur depleted conditions thereby implicating this abundant chemoautotroph in the cryptic marine sulfur cycle in oxygenated waters. But the role of SUP05 bacteria may vary dramatically depending on availability of oxygen. Within anaerobic environments, Ca. Thioglobus autotrophicus” are active reducers of nitrate. I estimate that anaerobic cells reduce approximately 0.36-0.84 fm N/cell/day whereas in aerobic environments, cells do not reduce any nitrate (Table 2). Protein expression data provides further evidence for a dramatic shift in metabolic activity in aerobic versus anaerobic ‘Ca. Thioglobus autotrophicus’. The complete absence of expression of putative nitrate reductase genes (nar) in aerobic cells shows that aerobic SUP05 do not contribute to the nitrogen cycle when using oxygen as an electron acceptor (Fig 5). Despite this, they do produce more biomass and fix more carbon in the presence of oxygen showing that their role in the environment must be reconsidered in relation to availability and use of oxygen as an electron acceptor.

3.6 REFERENCES

1. Anantharaman K, Breier JA, Sheik CS, Dick GJ. (2013). Evidence for hydrogen oxidation and metabolic plasticity in widespread deep-sea sulfur-oxidizing bacteria. *Proc Natl Acad Sci U S A* **110**: 330–5.
2. Anderson RE, Beltrán MT, Hallam SJ, Baross J a. (2013). Microbial community structure across fluid gradients in the Juan de Fuca Ridge hydrothermal system. *FEMS Microbiol Ecol* **83**: 324–39.
3. Aumonda V, Waelesa M, Salaünb P, Gibbon-Walsh K, van den Berg, Constant MG, Pierre-Marie S, *et al.* (2012). Sulfide determination in hydrothermal seawater samples using a vibrating gold micro-wire electrode in conjunction with stripping chronopotentiometry. *Anal Chim Acta* **753**: 42–47.
4. Canfield DE, Stewart FJ, Thamdrup B, De Brabandere L, Dalsgaard T, Delong EF, *et al.* (2010). A cryptic sulfur cycle in oxygen minimum zone waters off the Chilean coast. *Science (80-)* **330**: 1375–1378.
5. Dyksma S, Bischof K, Fuchs BM, Hoffmann K, Meier D, Meyerdierks A, *et al.* (2016). Ubiquitous Gammaproteobacteria dominate dark carbon fixation in coastal sediments. *ISME J* **10**: 1–15.
6. Glaubitz S, Kießlich K, Meeske C, Labrenz M, Jürgens K. (2013). SUP05 Dominates the gammaproteobacterial sulfur oxidizer assemblages in pelagic redoxclines of the central Baltic and Black seas. *Appl Environ Microbiol* **79**: 2767–2776.
7. Hawley AK, Brewer HM, Norbeck AD, Pasa-Tolic L, Hallam SJ. (2014). Metaproteomics reveals differential modes of metabolic coupling among ubiquitous oxygen minimum zone microbes. *Proc Natl Acad Sci* **111**: 11395–11400.
8. Iancu C V, Tivol WF, Schooler JB, Dias DP, Henderson GP, Murphy GE, *et al.* (2007). Electron cryotomography sample preparation using the Vitrobot. *Nat Protoc* **1**: 2813–2819.
9. Johnston DT, Gill BC, Masterson A, Beirne E, Casciotti KL, Knapp AN, *et al.* (2014). Placing an upper limit on cryptic marine sulphur cycling. *Nature* **513**: 530–533.
10. Kremer JR, Mastrorarde DN, McIntosh JR. (1996). Computer visualization of three-dimensional image data using IMOD. *J Struct Biol* **116**: 71–6.
11. Ksionzek KB, Ksionzek KB, Lechtenfeld OJ, Mccallister SL, Schmitt-kopplin P, Geuer JK, *et al.* (2016). Dissolved organic sulfur in the ocean : Biogeochemistry of a petagram inventory. **7796**.

12. Lavik G, Stuhmann T, Bruchert V, Van der Plas A, Mohrholtz V, Lam P, *et al.* (2009). Detoxification of sulphidic African shelf waters by blooming chemolithotrophs. *Nature* **457**: 581–584.
13. Maki JS. (2013). Bacterial intracellular sulfur globules: Structure and function. *J Mol Microbiol Biotechnol* **23**: 270–280. Marshall KT, Morris RM. (2012). Isolation of an aerobic sulfur oxidizer from the SUP05/Arctic96BD-19 clade. *ISME J* **7**: 452–455.
14. Mastrorade DN. (2005). Automated electron microscope tomography using robust prediction of specimen movements. *J Struct Biol* **152**: 36–51.
15. Mattes TE, Nunn BL, Marshall KT, Proskurowski G, Kelley DS, Kawka OE, *et al.* (2013). Sulfur oxidizers dominate carbon fixation at a biogeochemical hot spot in the dark ocean. *ISME J* **7**: 1–12.
16. Pruski AM, Medioni AF, Prodon R, Colomines JC. (2000). Thiotaurine is a biomarker of sulfide-based symbiosis in deep-sea bivalves. *Limnol Oceanogr* **45**: 1860–1867.
17. Reisch CR, Moran MA, Whitman WB. (2011). Bacterial catabolism of dimethylsulfoniopropionate (DMSP). *Front Microbiol* **2**: 1–12.
18. Rogge A, Vogts A, Voss M, Jürgens K, Jost G, Labrenz M. (2017). Success of chemolithoautotrophic SUP05 and Sulfurimonas GD17 cells in pelagic Baltic Sea redox zones is facilitated by their lifestyles as K- and r-strategists. *Environ Microbiol* **19**: 2495–2506.
19. Shah V, Chang BX, Morris RM. (2017). Cultivation of a chemoautotroph from the SUP05 clade of marine bacteria that produces nitrite and consumes ammonium. *ISME J* **11**: 1–9.
20. Sievert SM, Kiene RP, Schulz-vogt HN. (2007). The Sulfur Cycle. In: *A Sea of Microbes*. pp 117–123. Stevens H, Ulloa O. (2008). Bacterial diversity in the oxygen minimum zone of the eastern tropical South Pacific. *Environ Microbiol* **10**: 1244–1259.
21. Stewart FJ, Ulloa O, Delong EF. (2012). Microbial metatranscriptomics in a permanent marine oxygen minimum zone. *Environ Microbiol* **14**: 23–40.
22. Stramma L, Johnson GC, Sprintall J, Mohrholtz V. (2008). Expanding oxygen-minimum zones in the tropical oceans. *Science* **320**: 655–658.
23. Teske A. (2010). Oceans. Cryptic links in the ocean. *Science (80-)* **330**: 1326–7.
24. Ulloa O, Canfield DE, DeLong EF, Letelier RM, Stewart FJ. (2012). Microbial oceanography of anoxic oxygen minimum zones. *Proc Natl Acad Sci U S A* **109**: 15996–6003.
25. Walsh DA, Zaikova E, Howes CG, Song YC, Wright JJ, Tringe SG, *et al.* (2009). Metagenome of a versatile chemolithoautotroph from expanding oceanic dead zones. *Science*

- 326**: 578–582. Wright JJ, Konwar KM, Hallam SJ. (2012). Microbial ecology of expanding oxygen minimum zones. *Nat Rev Microbiol* **10**: 381–394.
26. Zaikova E, Walsh DA, Stilwell CP, Mohn WW, Tortell PD, Hallam SJ. (2010). Microbial community dynamics in a seasonally anoxic fjord: Saanich Inlet, British Columbia. *Environ Microbiol* **12**: 172–91.
27. Zhao X, Schwartz CL, Pierson J, Giovannoni SJ, McIntosh JR. (2017). Three-Dimensional Structure of the Ultraoligotrophic Marine Bacterium ‘Candidatus Pelagibacter ubique’. **83**: ‘1–14.

3.7 ACKNOWLEDGEMENT

Cell images and other data related to this project are archived online and available through The Biological and Chemical Oceanography Data Management Office (BCO-DMO). I thank Dr. Z. Chen for training and management of the UT Southwestern Medical Center Cryo-Electron Microscopy Facility. This work was funded in part by a grant from the National Science Foundation awarded to R. Morris and A. Ingalls (OCE-15584830). I would like to thank members of the Center for Environmental Genomics (CEG) at the University of Washington for their support and valuable feedback on the research and manuscript.

Table 3.1. Carbon, nitrogen and hydrogen content in “*Ca. T. autotrophicus*” cells grown under aerobic and anaerobic environments. See materials and methods for specifics regarding growth conditions and CHN analyses

| | Anaerobic | Aerobic | Aerobic/Anaerobic |
|--------------------|------------------|----------------|--------------------------|
| Carbon/cell (fg) | 9.9 | 32.2 | 3.25 |
| Nitrogen/cell (fg) | 2.29 | 9.3 | 4.06 |
| Hydrogen/cell (fg) | 0.11 | 1.6 | 9.63 |

Table 3.2. Physiological differences in “*Ca. T. autotrophicus*” cells grown under aerobic and anaerobic growth conditions. See materials and methods for specifics regarding growth conditions, cryo-electron tomography measurements and growth calculations.

| | Anaerobic | Aerobic |
|--|--------------------|------------------|
| ▲Cell diameter (μm) | 0.462 ± 0.032 | +-- |
| Cell volume (μm ³) | 0.056 ± 0.0092 | 0.22 ± 0.228 |
| Sulfur globule diameter (μm) | 0.156 ± 0.017 | 0.36 ± 0.162 |
| Sulfur globule volume (μm ³) | 0.00213 ± 0.000538 | 0.0305 ± 0.00243 |
| ●Specific growth rate | 0.024-0.058 | 0.035-0.080 |
| Doubling time (hours) | 11.90-28.11 | 8.60-19.81 |
| Carbon fixation (fM/cell/day) | 0.70-1.66 | 3.25-7.49 |
| Nitrate reduction (fM/cell/day) | 0.36-0.84 | -- |

▲Determined by cryo-electron tomography

●Calculated from growth experiments and CHN analyses

+ Not measurable due to variable cell shape

Figure 3.1. Final cell densities of “*Ca. Thioglobus autotrophicus*” on sulfur deplete media.

Aerobic and anaerobic growths of cultures in sulfur deplete media. First two bars indicate final cell density of inoculum and density at which cells were transferred (solid line). Subsequent bars represent 1st, 2nd and 3rd serial transfers of 10³ cells/mL into aerobic and anaerobic media with no sulfur amendments. Lower limit of y-axis set at the instrumental detection limit of cell count (10³). All experiments except ‘Inoculum’ were done in biological triplicates.

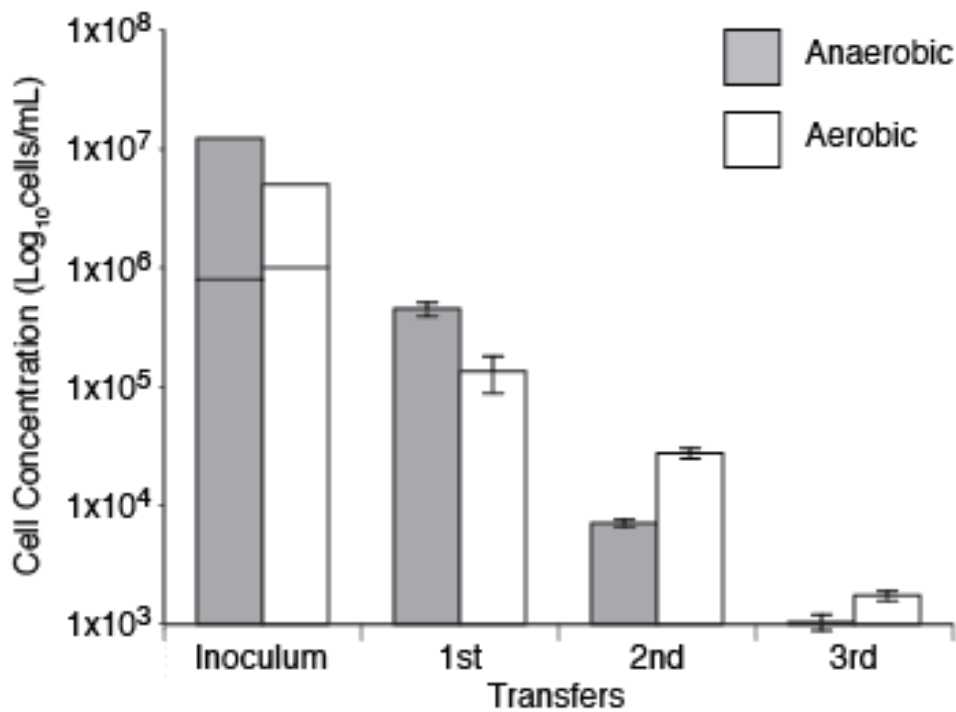


Figure 3.2. Cryo-electron tomography of intact frozen-hydrated “Ca. *Thioglobus autotrophicus*” cells under various growth conditions. (A-D) Tomographic slices of 3D reconstructed *T. autotrophicus* cells grown under (A) anaerobic condition (-O₂) with sulfur source present (+S), (B) anaerobic condition without sulfur source in the medium (-S), (C) aerobic condition (+O₂) without sulfur source, and (D) aerobic condition with sulfur source. All cells grown with a sulfur source present store electron-dense sulfur globule(s) (yellow arrows) in their periplasmic space, i.e. between their inner and outer membrane (IM, OM). Note that all cells are displayed at the same scale (scale bar in D: 200 nm), which demonstrates that cells cultured aerobically with sulfur present (D) grow to a significantly larger size, and store multiple and/or larger sulfur granules than cells grown anaerobically (A). Other labels: N, nucleoid; arrowheads, ribosome-sized particles. The cell in (D) is so large that the edges of the camera field of view were visible in the image corners, which have been faded into a gray background.

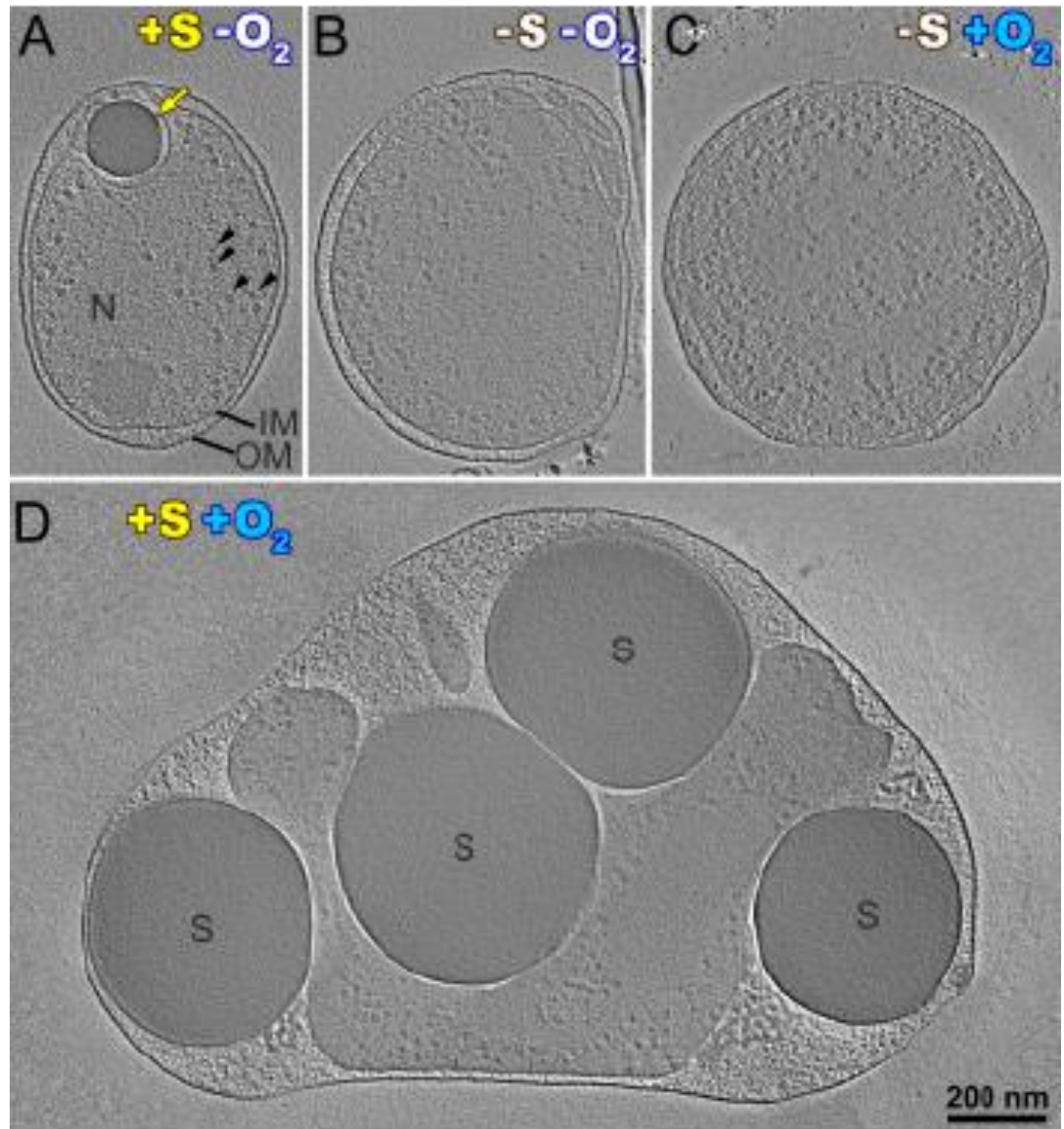


Figure 3.3. Specific growth rate and final cell densities of “*Ca. Thioglobus autotrophicus*” on Sulfide, Thiosulfate and Thiotaaurine. (A) Specific growth rate under anaerobic conditions and (B) Final cell density in media enriched with 0.01,0.1,1,10 and 100 μM of Sulfide, Thiosulfate and Thiotaaurine. Lower limit of y-axis is set at the instrumental detection limit of cell count (10^3) All experiments were done in triplicates.

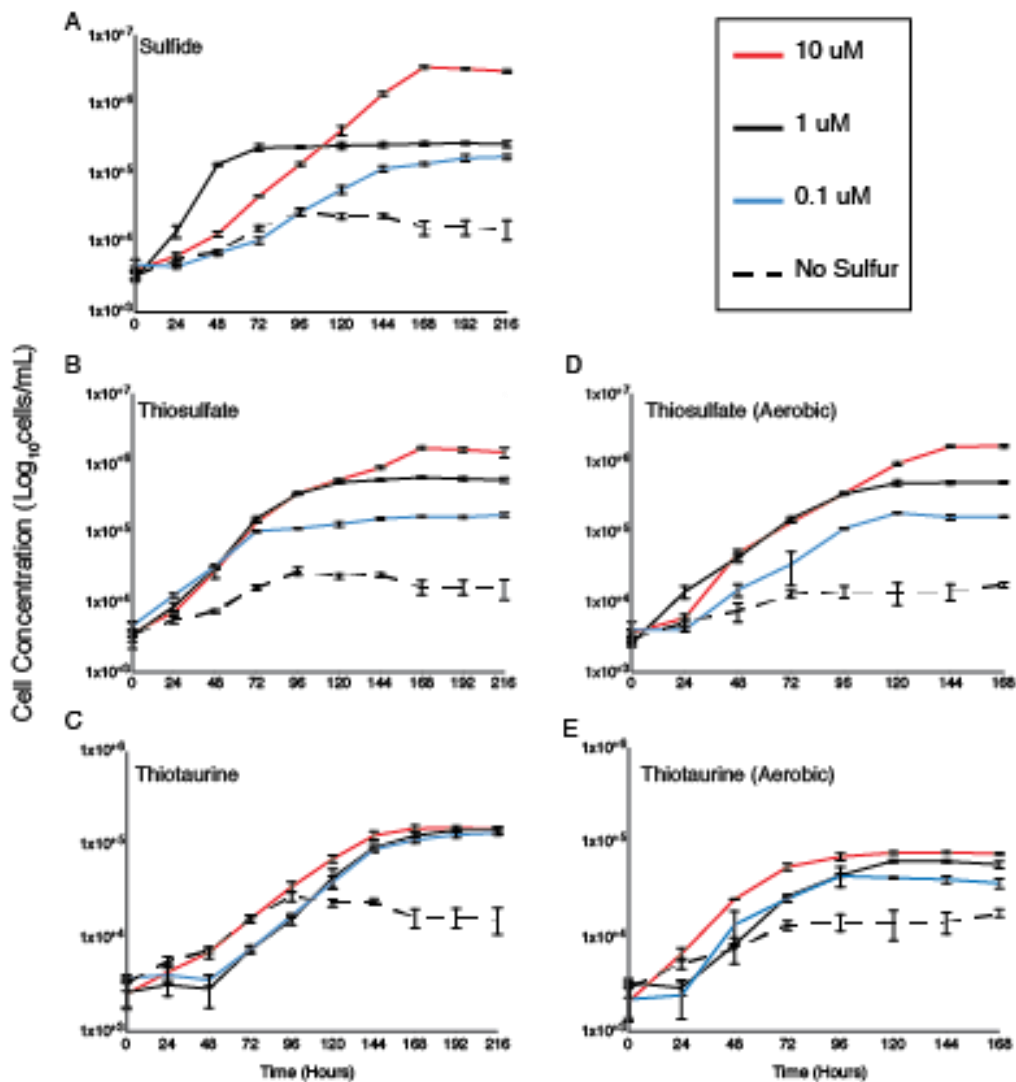


Figure 3.4. Protein expression in “*Ca. Thioglobus autotrophicus*” during aerobic and anaerobic growth. Proteins related to carbon metabolism (orange), dissimilatory nitrogen metabolism (dark blue), assimilatory nitrogen metabolism (light blue) and sulfur metabolism (dark gray). Bubble plots indicate abundance of select protein (abbreviated names with accession number) in aerobic versus anaerobic treatments. Log 2 fold change bar plots show the differences between the two treatments.

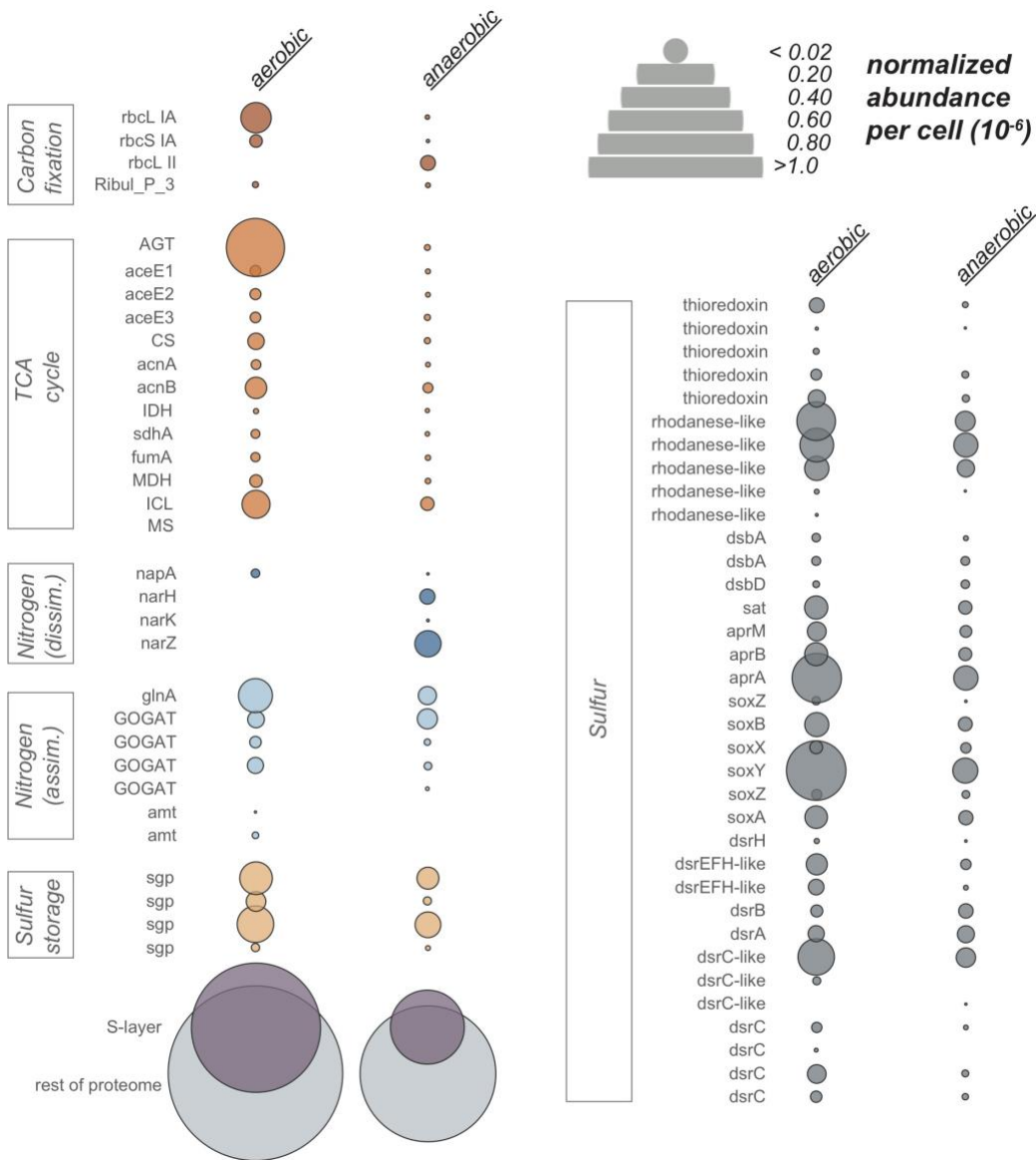
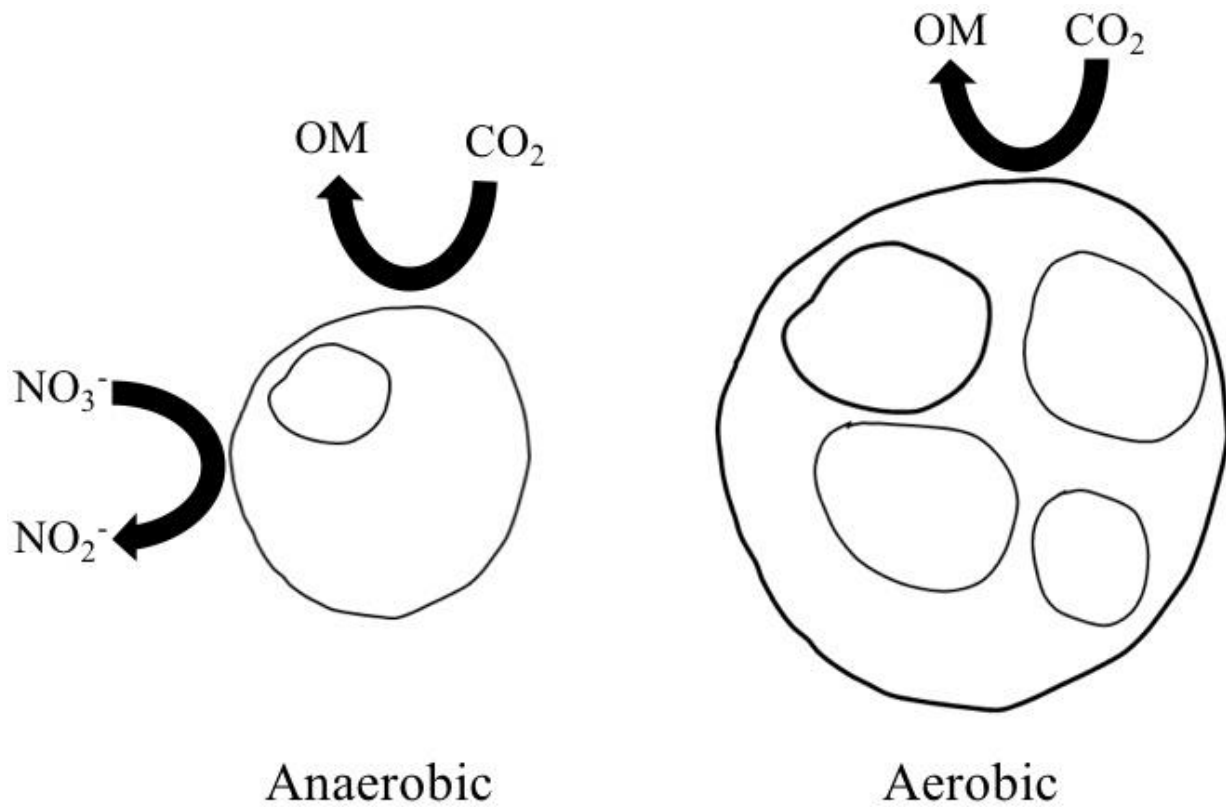
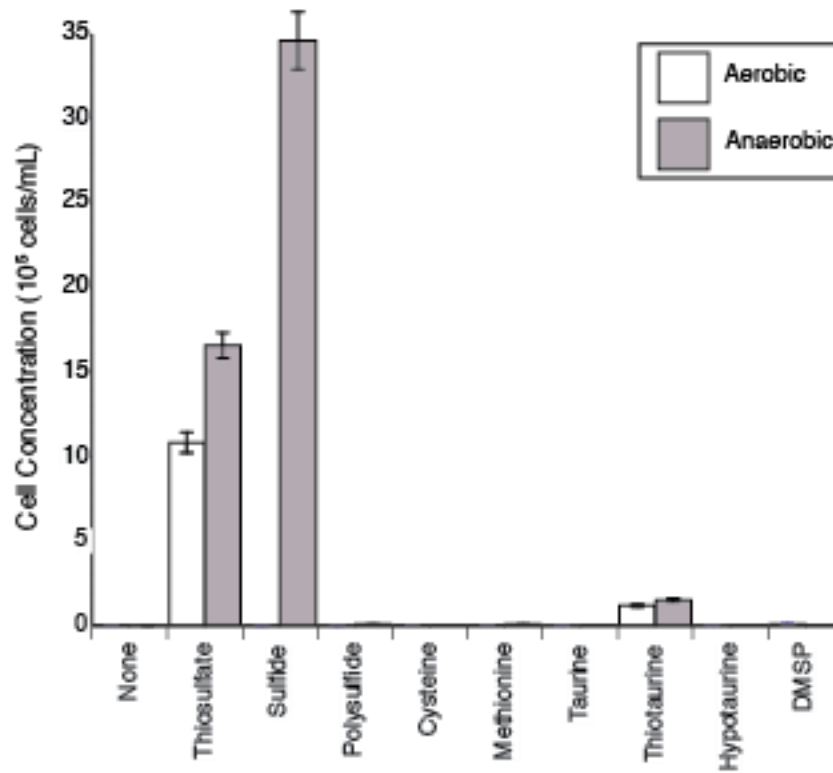


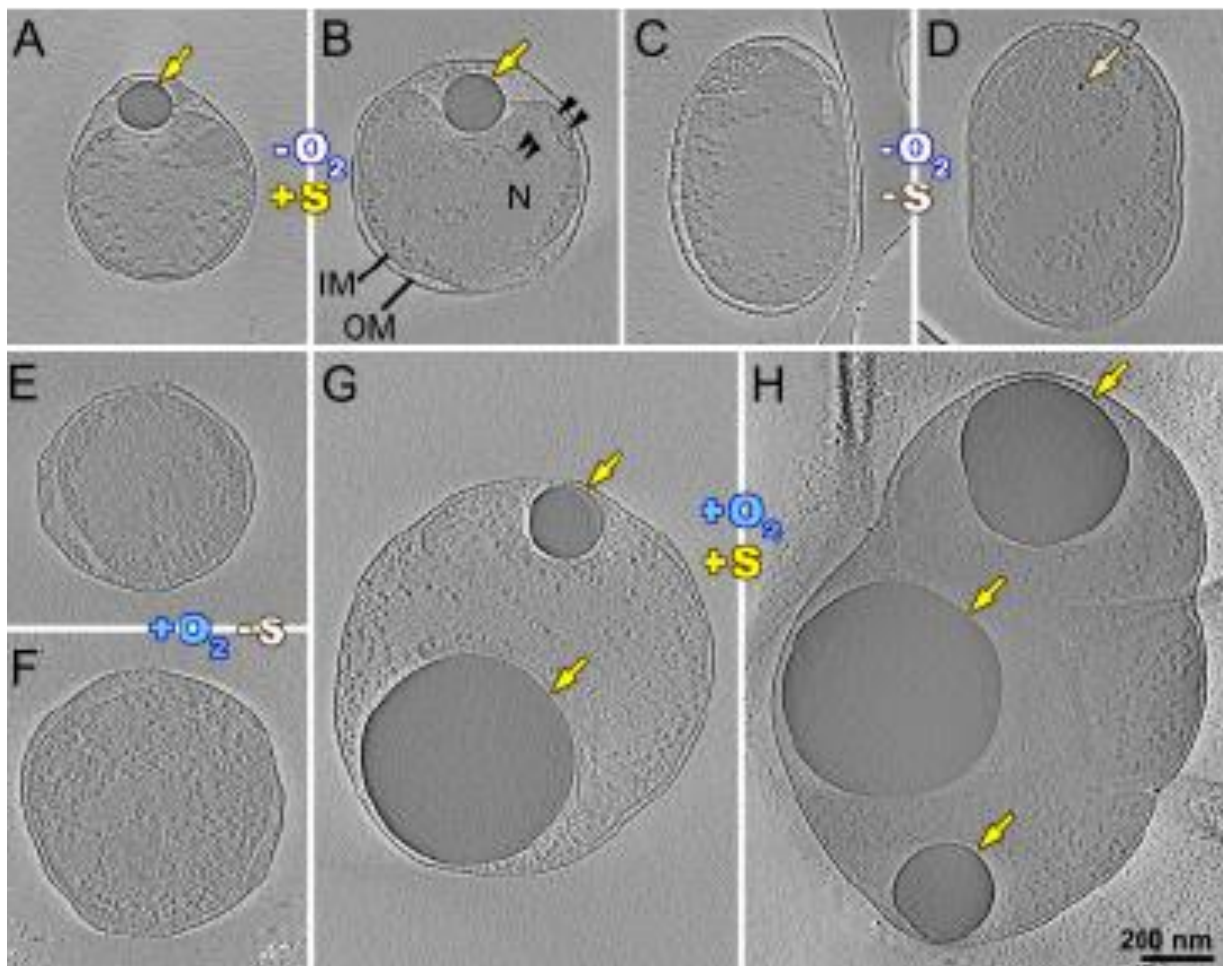
Figure 3.5. Proposed role of SUP05 bacteria in aerobic and anaerobic environments. A) Theoretical models showing a typical anaerobic cell with arrows showing influx and out put of nitrogen and carbon. B) A typical aerobic cell with arrows showing influx and output of carbon.



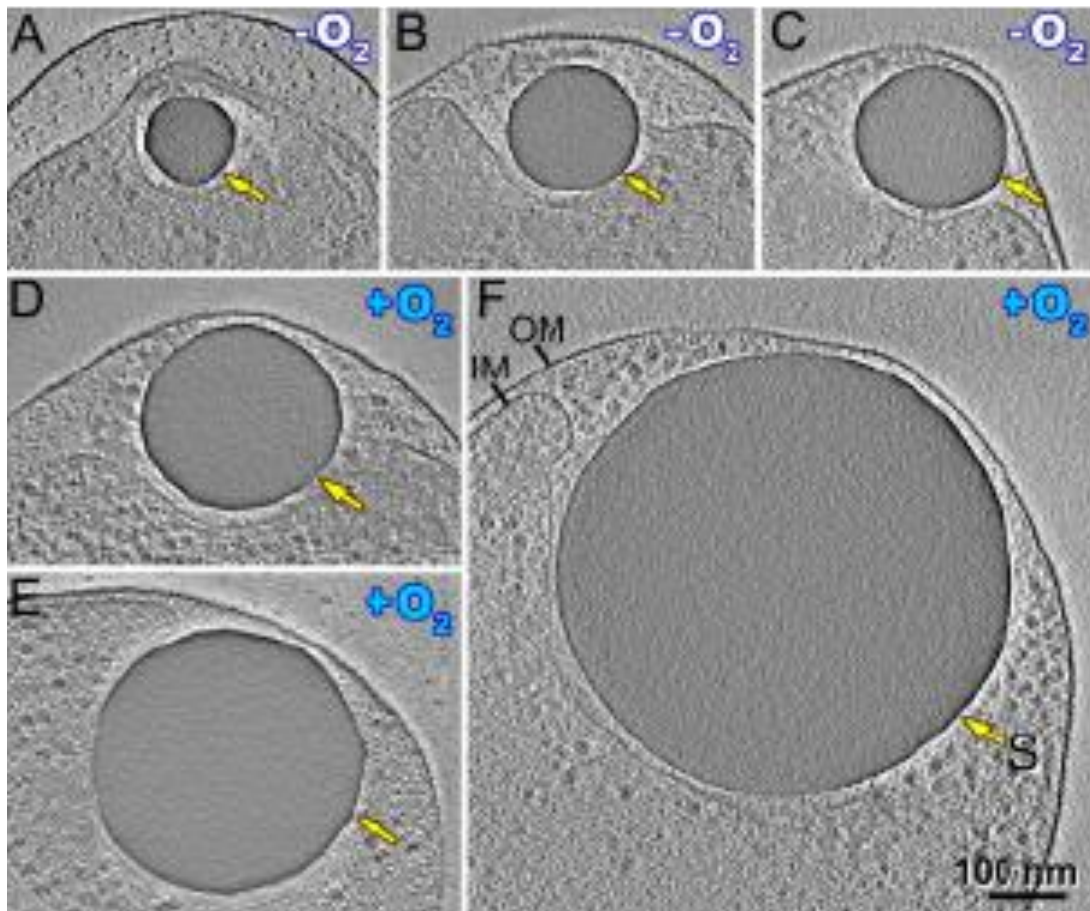
Supplementary Figure 3.1. Final cell densities of “*Ca. Thioglobus autotrophicus*” on Organic and Inorganic Sulfur. Aerobic and anaerobic growth of cells in 10 μ M of inorganic reduced sulfur compounds (Thiosulfate, Sulfide & Polysulfide) and organic reduced sulfur compounds (Cysteine, Methionine, Taurine, Thiotaurine, Hypotaurine & DMSP). All experiments were conducted in biological triplicates.



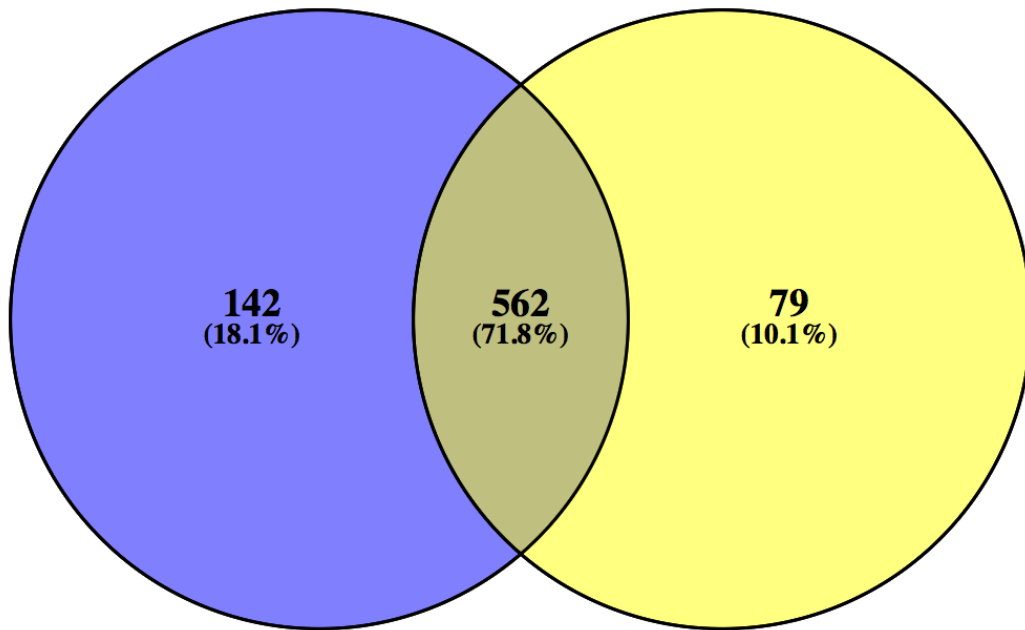
Supplementary Figure 3.2. Cryo-ET reconstructed intact frozen-hydrated “Ca. *Thioglobus autotrophicus*” cells are shown for the four different growth conditions; relates to Fig. 1. (A-H) Tomographic slices of 3D reconstructed *T. autotrophicus* cells cultured under (A,B) anaerobic condition (-O₂) with sulfur source present (+S), (C,D) anaerobic condition without sulfur source in the medium (-S), (E,F) aerobic condition (+O₂) without sulfur source, and (G,H) aerobic condition with sulfur source. All cells are displayed at the same scale (scale bar in H: 200 nm); cells grown with a sulfur source present store electron-dense sulfur globule(s) (yellow arrows) in their periplasmic space, i.e. between their inner and outer membrane (IM, OM). Other labels: N, nucleoid; arrowheads, ribosome-sized particles. It is not clear if the electron-dense particle in (D) is a nascent/remnant of a sulfur granule (light yellow arrow;).



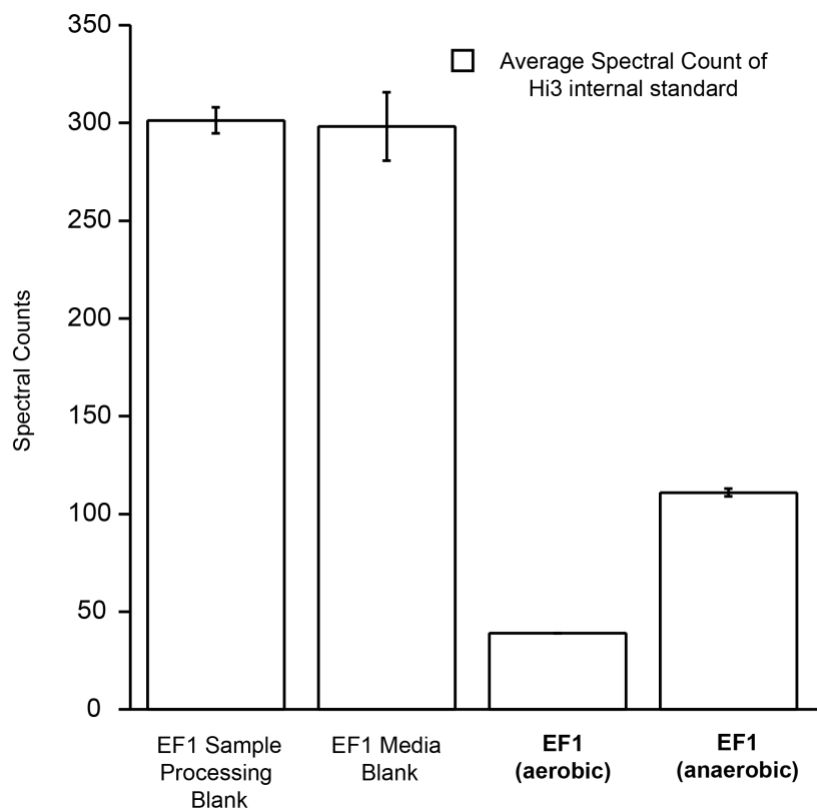
Supplementary Figure 3.3. Range of sizes of sulfur globules within “Ca. *Thioglobus autotrophicus*” cells. (A-F) Tomographic slices at higher magnification show the 3D reconstructed sulfur globules (yellow arrows) in *T. autotrophicus* cells cultured with a sulfur source present in the medium. However, under (A-C) anaerobic conditions (-O₂) the sulfur globules were smaller than under (D-F) aerobic conditions (+O₂). Other labels: IM, inner membrane; OM, outer membrane; S, sulfur globule (yellow arrows). All images are displayed at the same scale (scale bar in F: 100 nm).



Supplementary Figure 3.4 Venn diagram comparing the number observed proteins shared between EF1 growth conditions, corresponding to >95% protein probability and following data constraints. EF1 grown aerobically (blue) and EF1 grown anaerobically (yellow). All 22 proteins observed in media blank were shared between EF1 conditions.



Supplementary Figure 3.5 Matrix effect analysis of Hi3 internal standard peptides as reported in averaged spectral counts (with standard deviation reported as error bars) for triplicate injections. Hi3 internal standard was resuspended at an identical concentration for each sample and injected as 100 fmol on-column. Bar graphs represent data from EF1 (aerobic) compared to EF1 (anaerobic) along with a corresponding sample processing control (only AMBIC/EDTA buffer) and media blank control



Supplementary Table 3.1. Specific growth rates and highest cell yield of “*Ca. Thioglobus autotrophicus*” on Sulfide, Thiosulfate and Thiotaurine over a range of substrate concentrations

| Substrate Concentration (μM) | Anaerobic | | | Aerobic | | |
|------------------------------|---|-------------------|---|---|-------------------|---|
| | Specific Growth Rate (h ⁻¹) | Doubling Time (h) | Highest Cell Yield (cells/mL) | Specific Growth Rate (h ⁻¹) | Doubling Time (h) | Highest Cell Yield (cells/mL) |
| THIOSULFATE | | | | | | |
| 0.01 | 0.038 ± 0.005 | 18 | 1.94x10 ⁵ ± 7.06x10 ³ □ | 0.031 ± 0.001 | 18 | 5.77x10 ⁴ ± 2.08x10 ⁴ □ |
| 0.1 | 0.044 ± 0.002 | 15 | 1.81x10 ⁵ ± 1.18x10 ⁴ | 0.043 ± 0.012 | 16 | 1.93x10 ⁵ ± 9.21x10 ⁴ |
| 1 | 0.051 ± 0.001 | 13 | 6.25x10 ⁵ ± 2.19x10 ⁴ | 0.044 ± 0.004 | 15 | 5.30x10 ⁵ ± 2.57x10 ⁴ |
| 10 | 0.054 ± 0.004 | 12 | 1.66x10 ⁶ ± 7.62x10 ⁴ | 0.066 ± 0.003 | 10 | 1.77x10 ⁶ ± 5.49x10 ⁴ |
| 100 | 0.057 ± 0.001* | 12 | 3.70x10 ⁶ ± 1.14x10 ⁵ | 0.081 ± 0.007* | 8 | 2.68x10 ⁶ ± 2.67x10 ⁴ |
| THIOTAURINE | | | | | | |
| 0.01 | 0.032 ± 0.007 | 21 | 1.13x10 ⁵ ± 1.34x10 ⁴ □ | 0.035 ± 0.003 | 19 | 4.32x10 ⁵ ± 4.27x10 ³ □ |
| 0.1 | 0.035 ± 0.005 | 20 | 1.35x10 ⁵ ± 6.44x10 ³ | 0.042 ± 0.009 | 13 | 4.42x10 ⁵ ± 1.38x10 ³ |
| 1 | 0.037 ± 0.007 | 18 | 1.45x10 ⁵ ± 6.94x10 ³ | 0.047 ± 0.004* | 14 | 6.38x10 ⁵ ± 2.01x10 ³ |
| 10 | 0.034 ± 0.001 | 20 | 1.52x10 ⁶ ± 7.03x10 ³ | 0.044 ± 0.002 | 15 | 7.83x10 ⁶ ± 3.77x10 ⁴ |
| 100 | 0.046 ± 0.003* | 15 | 8.40x10 ⁶ ± 4.50x10 ⁴ | 0.042 ± 0.007 | 16 | 2.09x10 ⁶ ± 5.29x10 ⁴ |
| SULFIDE | | | | | | |
| 0.01 | 0.025 ± 0.005 | 28 | 1.37x10 ⁵ ± 8.37x10 ³ □ | | | |
| 0.1 | 0.035 ± 0.005 | 19 | 1.75x10 ⁵ ± 1.28x10 ⁴ | | | |
| 1 | 0.058 ± 0.004* | 11 | 2.75x10 ⁵ ± 1.08x10 ⁴ | | | &NA |
| 10 | 0.049 ± 0.001 | 14 | 3.46x10 ⁶ ± 1.70x10 ⁵ | | | |
| 100 | 0.028 ± 0.007 | 24 | 3.26x10 ⁴ ± 4.98x10 ³ | | | |

* Highest value within the series

&No data for aerobic growth on sulfide due interference from abiotic oxidation

Supplementary Table 3.2. Accession Numbers and description of expressed proteins in “*Ca. Thioglobus autotrophicus*” aerobic and anaerobic cells

| Gene Number | Protein Description | Averaged normalized spectral counts-adjusted PER CELL (T.autotrophicus Aerobic) | Averaged normalized spectral counts-adjusted PER CELL (T.autotrophicus Anaerobic) |
|----------------------|--|---|---|
| S-layer (SP60_01315) | A0A0M4NW98_9GAMM Uncharacterized protein OS=Candidatus Thioglobus autotrophicus GN=SP60_01315 PE=4 SV=1 | 5.47E-07 | 1.79E-07 |
| sgp (SP60_03970) | A0A0M4NTK9_9GAMM Uncharacterized protein OS=Candidatus Thioglobus autotrophicus GN=SP60_03970 PE=4 SV=1 | 2.27E-09 | 7.69E-10 |
| sgp (SP60_00735) | A0A0M4PM17_9GAMM Uncharacterized protein OS=Candidatus Thioglobus autotrophicus GN=SP60_00735 PE=4 SV=1 | 4.39E-08 | 2.17E-08 |
| sgp (SP60_00730) | A0A0M5LEB6_9GAMM Uncharacterized protein OS=Candidatus Thioglobus autotrophicus GN=SP60_00730 PE=4 SV=1 | 1.27E-08 | 2.19E-09 |
| sgp (SP60_00725) | A0A0M4NW56_9GAMM Uncharacterized protein OS=Candidatus Thioglobus autotrophicus GN=SP60_00725 PE=4 SV=1 | 3.49E-08 | 1.58E-08 |
| narZ (SP60_06775) | A0A0M3TUH3_9GAMM Nitrate reductase OS=Candidatus Thioglobus autotrophicus GN=narZ PE=3 SV=1 | | 2.26E-08 |

| | | | |
|-------------------------|---|----------|----------|
| narK (SP60_06765) | A0A0M4NYP6_9GAMM Major facilitator transporter OS=Candidatus Thioglobus autotrophicus GN=SP60_06765 PE=4 SV=1 | | 2.63E-10 |
| narH (SP60_06780) | A0A0M4NJP2_9GAMM Nitrate reductase OS=Candidatus Thioglobus autotrophicus GN=narH PE=4 SV=1 | | 7.57E-09 |
| napA (SP60_01840) | A0A0M4NI36_9GAMM Nitrate reductase OS=Candidatus Thioglobus autotrophicus GN=SP60_01840 PE=4 SV=1 | 2.44E-09 | 2.02E-10 |
| amt (SP60_05835) | A0A0M3TUE1_9GAMM Ammonium transporter OS=Candidatus Thioglobus autotrophicus GN=SP60_05835 PE=4 SV=1 | 1.44E-09 | |
| amt (SP60_05805) | A0A0M3TU78_9GAMM Ammonium transporter OS=Candidatus Thioglobus autotrophicus GN=SP60_05805 PE=3 SV=1 | 1.66E-10 | |
| GOGAT (SP60_06975) | A0A0M4NHX2_9GAMM Glutamate synthase OS=Candidatus Thioglobus autotrophicus GN=SP60_06975 PE=3 SV=1 | | 4.65E-10 |
| GOGAT (SP60_03575) | A0A0M4NWW3_9GAMM Glutamate synthase OS=Candidatus Thioglobus autotrophicus GN=SP60_03575 PE=4 SV=1 | 8.52E-09 | 1.98E-09 |
| GOGAT (SP60_01875) | A0A0M3TU06_9GAMM Glutamate synthase OS=Candidatus Thioglobus autotrophicus GN=SP60_01875 PE=4 SV=1 | 4.37E-09 | 1.36E-09 |
| GOGAT (SP60_01830) | A0A0M5LEE9_9GAMM Glutamate synthase OS=Candidatus Thioglobus autotrophicus GN=SP60_01830 PE=4 SV=1 | 9.13E-09 | 1.33E-08 |
| glnA (SP60_00180) | A0A0M3TTN7_9GAMM Glutamine synthetase OS=Candidatus Thioglobus autotrophicus GN=glnA PE=3 SV=1 | 3.79E-08 | 1.08E-08 |
| rbcS IA (SP60_06730) | A0A0M4PNW9_9GAMM Ribulose 1,5-bisphosphate carboxylase small subunit OS=Candidatus Thioglobus autotrophicus GN=SP60_06730 PE=4 SV=1 | 5.20E-09 | 3.84E-10 |

| | | | |
|--------------------------------|---|----------|----------|
| rbcL IA (SP60_06725) | A0A0M5LJD8_9GAMM Ribulose 1,5-bisphosphate carboxylase OS=Candidatus Thioglobus autotrophicus GN=rbcL PE=3 SV=1 | 3.04E-08 | 6.68E-10 |
| rbcL II (SP60_06705) | A0A0M4PL98_9GAMM Ribulose 1,5-bisphosphate carboxylase OS=Candidatus Thioglobus autotrophicus GN=SP60_06705 PE=3 SV=1 | | 7.26E-09 |
| Ribul_P_3_epim (SP60_03910) | A0A0M3TU71_9GAMM Ribulose- phosphate 3-epimerase OS=Candidatus Thioglobus autotrophicus GN=SP60_03910 PE=3 SV=1 | 1.22E-09 | 7.89E-10 |
| ICL (SP60_01905) | A0A0M4NI43_9GAMM Isocitrate lyase OS=Candidatus Thioglobus autotrophicus GN=SP60_01905 PE=4 SV=1 | 2.57E-08 | 5.93E-09 |
| MDH (SP60_05970) | A0A0M4NJE7_9GAMM Malate dehydrogenase OS=Candidatus Thioglobus autotrophicus GN=SP60_05970 PE=4 SV=1 | 5.20E-09 | 1.01E-09 |
| fumA (SP60_06140) | A0A0M4NX39_9GAMM Fumarate hydratase class I OS=Candidatus Thioglobus autotrophicus GN=SP60_06140 PE=3 SV=1 | 2.82E-09 | 9.51E-10 |
| sdhA (SP60_05960) | A0A0M5LEM4_9GAMM Succinate dehydrogenase OS=Candidatus Thioglobus autotrophicus GN=sdhA PE=4 SV=1 | 2.60E-09 | 6.68E-10 |
| IDH (SP60_00740) | A0A0M3TTW8_9GAMM Isocitrate dehydrogenase [NADP] OS=Candidatus Thioglobus autotrophicus GN=SP60_00740 PE=3 SV=1 | 8.86E-10 | 6.07E-10 |
| acnB (SP60_03270) | A0A0M4PMR6_9GAMM Aconitate hydratase B OS=Candidatus Thioglobus autotrophicus GN=SP60_03270 PE=3 SV=1 | 1.51E-08 | 3.30E-09 |
| acnA (SP60_00885) | A0A0M4PM28_9GAMM Aconitate hydratase OS=Candidatus Thioglobus autotrophicus GN=SP60_00885 PE=3 SV=1 | 3.10E-09 | 7.49E-10 |

| | | | |
|------------------------|--|----------|----------|
| CS (SP60_00890) | A0A0M4NV11_9GAMM Citrate synthase OS=Candidatus Thioglobus autotrophicus GN=SP60_00890 PE=3 SV=1 | 8.86E-09 | 1.25E-09 |
| aceE3 (SP60_03105) | A0A0M4NK87_9GAMM Dihydrolipoyl dehydrogenase OS=Candidatus Thioglobus autotrophicus GN=SP60_03105 PE=4 SV=1 | 3.71E-09 | 1.23E-09 |
| aceE2 (SP60_03100) | A0A0M4PLU5_9GAMM Dihydrolipoamide acetyltransferase component of pyruvate dehydrogenase complex OS=Candidatus Thioglobus autotrophicus GN=SP60_03100 PE=3 SV=1 | 3.99E-09 | 7.49E-10 |
| aceE1 (SP60_00440) | A0A0M4NSN7_9GAMM Pyruvate dehydrogenase E1 component OS=Candidatus Thioglobus autotrophicus GN=aceE PE=4 SV=1 | 3.82E-09 | 8.09E-10 |
| AGT (SP60_01480) | A0A0M4NHZ4_9GAMM Alanine--glyoxylate aminotransferase OS=Candidatus Thioglobus autotrophicus GN=SP60_01480 PE=3 SV=1 | 1.11E-07 | 1.13E-09 |
| dsrC (SP60_07540) | A0A0M3TUP2_9GAMM Sulfurtransferase OS=Candidatus Thioglobus autotrophicus GN=SP60_07540 PE=4 SV=1 | 4.26E-09 | 1.34E-09 |
| dsrC (SP60_07285) | A0A0M4PLG6_9GAMM Sulfurtransferase OS=Candidatus Thioglobus autotrophicus GN=SP60_07285 PE=3 SV=1 | 1.15E-08 | 1.58E-09 |
| dsrC (SP60_03695) | A0A0M4PKF3_9GAMM Sulfur relay protein DsrC OS=Candidatus Thioglobus autotrophicus GN=SP60_03695 PE=4 SV=1 | 4.98E-10 | |
| dsrC (SP60_01550) | A0A0M4NWB8_9GAMM Pyridine nucleotide-disulfide oxidoreductase OS=Candidatus Thioglobus autotrophicus GN=SP60_01550 PE=4 SV=1 | 3.49E-09 | 7.28E-10 |
| dsrC-like (SP60_06795) | A0A0M3TUP0_9GAMM Sulfurtransferase OS=Candidatus Thioglobus autotrophicus GN=SP60_06795 PE=3 SV=1 | | 1.82E-10 |

| | | | |
|-----------------------------|--|----------|----------|
| dsrC-like (SP60_01955) | A0A0M4P881_9GAMM Sulfurtransferase OS=Candidatus Thioglobus autotrophicus GN=SP60_01955 PE=3 SV=1 | 2.10E-09 | |
| dsrC-like (SP60_01845) | A0A0M4NWE7_9GAMM Sulfurtransferase OS=Candidatus Thioglobus autotrophicus GN=SP60_01845 PE=3 SV=1 | 4.36E-08 | 1.24E-08 |
| dsrA (SP60_01870) | A0A0M4NT22_9GAMM Sulfite reductase OS=Candidatus Thioglobus autotrophicus GN=SP60_01870 PE=4 SV=1 | 8.58E-09 | 9.53E-09 |
| dsrB (SP60_01865) | A0A0M4NVR9_9GAMM Sulfite reductase OS=Candidatus Thioglobus autotrophicus GN=SP60_01865 PE=4 SV=1 | 4.76E-09 | 6.84E-09 |
| dsrEFH-like (SP60_01860) | A0A0M4PMC3_9GAMM Sulfurtransferase OS=Candidatus Thioglobus autotrophicus GN=SP60_01860 PE=3 SV=1 | 8.03E-09 | 7.49E-10 |
| dsrEFH-like (SP60_01855) | A0A0M3TTU1_9GAMM Sulfur oxidoreductase OS=Candidatus Thioglobus autotrophicus GN=SP60_01855 PE=3 SV=1 | 1.46E-08 | 3.56E-09 |
| dsrH (SP60_01850) | A0A0M5LED8_9GAMM Multidrug MFS transporter OS=Candidatus Thioglobus autotrophicus GN=SP60_01850 PE=4 SV=1 | 8.86E-10 | 2.23E-10 |
| soxA (SP60_06060) | A0A0M4NXL5_9GAMM SoxAX cytochrome complex subunit A OS=Candidatus Thioglobus autotrophicus GN=SP60_06060 PE=3 SV=1 | 1.67E-08 | 6.62E-09 |
| soxZ (SP60_06055) | A0A0M3TU85_9GAMM Sulfur oxidation protein OS=Candidatus Thioglobus autotrophicus GN=SP60_06055 PE=4 SV=1 | 3.38E-09 | 1.98E-09 |
| soxY (SP60_06050) | A0A0M4NJF5_9GAMM Sulfur oxidation protein SoxY OS=Candidatus Thioglobus autotrophicus GN=SP60_06050 PE=4 SV=1 | 1.16E-07 | 2.07E-08 |
| soxX (SP60_06045) | A0A0M4PL68_9GAMM Cytochrome Cbb3 OS=Candidatus Thioglobus autotrophicus GN=SP60_06045 PE=4 SV=1 | 5.42E-09 | 3.56E-09 |

| | | | |
|----------------------|--|----------|----------|
| soxB (SP60_05195) | A0A0M4NJ63_9GAMM 5'-nucleotidase OS=Candidatus Thioglobus autotrophicus GN=SP60_05195 PE=3 SV=1 | 1.90E-08 | 6.33E-09 |
| soxZ (SP60_04810) | A0A0M5LEK8_9GAMM Uncharacterized protein OS=Candidatus Thioglobus autotrophicus GN=SP60_04810 PE=4 SV=1 | 2.27E-09 | 2.23E-10 |
| aprA (SP60_04590) | A0A0M4NX64_9GAMM Adenylylsulfate reductase OS=Candidatus Thioglobus autotrophicus GN=SP60_04590 PE=4 SV=1 | 7.98E-08 | 1.93E-08 |
| aprB (SP60_04585) | A0A0M3TU33_9GAMM Adenylylsulfate reductase OS=Candidatus Thioglobus autotrophicus GN=SP60_04585 PE=4 SV=1 | 1.73E-08 | 5.50E-09 |
| aprM (SP60_04580) | A0A0M4NIE9_9GAMM Adenylylsulfate reductase OS=Candidatus Thioglobus autotrophicus GN=SP60_04580 PE=4 SV=1 | 1.17E-08 | 4.59E-09 |
| sat (SP60_04575) | A0A0M4NIX4_9GAMM Sulfate adenylyltransferase OS=Candidatus Thioglobus autotrophicus GN=sat PE=3 SV=1 | 1.77E-08 | 5.79E-09 |
| dsbD (SP60_03840) | A0A0M5LL12_9GAMM Thiol:disulfide interchange protein DsbD OS=Candidatus Thioglobus autotrophicus GN=dsbD PE=3 SV=1 | 1.49E-09 | 2.41E-09 |
| dsbA (SP60_03800) | A0A0M5LJ66_9GAMM Pyridine nucleotide-disulfide oxidoreductase OS=Candidatus Thioglobus autotrophicus GN=SP60_03800 PE=4 SV=1 | 2.66E-09 | 2.57E-09 |
| dsbA (SP60_03070) | A0A0M5LET3_9GAMM Thiol:disulfide interchange protein OS=Candidatus Thioglobus autotrophicus GN=SP60_03070 PE=3 SV=1 | 2.38E-09 | 7.89E-10 |

| | | | |
|---------------------------|---|----------|----------|
| rhod-like (SP60_03470) | A0A0M4NWW5_9GAMM Sulfurtransferase OS=Candidatus Thioglobus autotrophicus GN=SP60_03470 PE=4 SV=1 | 2.77E-10 | |
| rhod-like (SP60_02965) | A0A0M4NWQ0_9GAMM Sulfurtransferase OS=Candidatus Thioglobus autotrophicus GN=SP60_02965 PE=4 SV=1 | 7.75E-10 | 1.62E-10 |
| rhod-like (SP60_01120) | A0A0M4NSV9_9GAMM Uncharacterized protein OS=Candidatus Thioglobus autotrophicus GN=SP60_01120 PE=4 SV=1 | 1.94E-08 | 9.83E-09 |
| rhod-like (SP60_01115) | A0A0M4NVK3_9GAMM Uncharacterized protein OS=Candidatus Thioglobus autotrophicus GN=SP60_01115 PE=4 SV=1 | 3.74E-08 | 1.91E-08 |
| rhod-like (SP60_01110) | A0A0M4PM49_9GAMM Uncharacterized protein OS=Candidatus Thioglobus autotrophicus GN=SP60_01110 PE=4 SV=1 | 4.89E-08 | 1.30E-08 |
| trx (SP60_06625) | A0A0M4NXS5_9GAMM Thioredoxin OS=Candidatus Thioglobus autotrophicus GN=SP60_06625 PE=3 SV=1 | 9.74E-09 | 1.76E-09 |
| trx (SP60_04250) | A0A0M4NH39_9GAMM Thioredoxin reductase OS=Candidatus Thioglobus autotrophicus GN=SP60_04250 PE=3 SV=1 | 3.87E-09 | 1.60E-09 |
| trx (SP60_03480) | A0A0M3TU56_9GAMM Thioredoxin OS=Candidatus Thioglobus autotrophicus GN=SP60_03480 PE=4 SV=1 | 1.22E-09 | |
| trx (SP60_00625) | A0A0M5LEI7_9GAMM Thioredoxin OS=Candidatus Thioglobus autotrophicus GN=SP60_00625 PE=4 SV=1 | 3.32E-10 | 1.62E-10 |
| trx (SP60_00300) | A0A0M3TTP1_9GAMM Thioredoxin OS=Candidatus Thioglobus autotrophicus GN=SP60_00300 PE=3 SV=1 | 7.25E-09 | 1.11E-09 |

CONCLUSION

Since the discovery of SUP05 bacteria, their role in the nitrogen cycle has been hotly debated. Several prominent studies suggested that SUP05 were involved in the removal of nitrogen via denitrification or DNRA (dissimilatory nitrate reduction to ammonia). In chapter 2, I show that ‘*Ca. Thioglobus autotrophicus*’ cells deviate from the previously believed roles. Although involved in the removal of nitrogen cycle, they only reduce nitrate to nitrite, thereby contributing to the large pool of nitrite at OMZs. In addition, they contain the genes for conversion of one particular intermediate of denitrification, nitric oxide to nitrous oxide. This is a rare instance of a marine OMZ organism possessing a truncated denitrification chain.

Ultimately, to better understand the activity of SUP05 in the environment, their role in multiple elemental cycles (C, N, S) needs to be better defined. Previous studies have focused entirely on their role in low oxygen marine environments despite evidence that they can utilize oxygen as an electron acceptor. In chapter 3, I use a growth experiments, imaging and protein expression to better classify the activity of *T.autotrophicus* in both aerobic and anaerobic environments and also to quantify the fluxes of carbon and nitrogen mediated by cells. Data obtained from *T.autotrophicus* cells provides evidence that the role of SUP05 cells in OMZs is not as previously predicted and has several nuances. I found that *T.autotrophicus* cells thrive in oxygenated water and can boost their sulfur and carbon storage several fold when they can access to oxygen. Growth experiments were also supported by protein expression data that show drastic changes in key proteins involved in cycling of carbon, nitrogen, sulfur across the oxic/anoxic interface. Laboratory based growth constraints of ‘*Ca. Thioglobus autotrophicus*’ cells provide a model for the types of environments that are viable habitats for SUP05. In

addition, the identification and quantification of highly conserved and highly expressed proteins can prove useful environmental markers/proxies for SUP05 abundance and activity.

The experiments and data analysis yield several novel discoveries. These include, the culture of a novel species, '*Ca. Thioglobus autotrophicus*', new information about its activity in the nitrogen cycle, discovery of a rare instance of a free living microbe that uses an organic source of sulfur (thiotaurine) for dissimilatory sulfur oxidization, formation of intracellular sulfur globules and the effect of oxygen on a well known low oxygen bacterium.

APPENDIX A

Table AppA.1 Comparison of percent yield of genomic DNA from three different commonly used DNA extraction methods

| DNA Estimate | Qiagen Kit | PowerSoil Kit | Phenoi Chloroform |
|---|--------------------|----------------------|--------------------------|
| Cells/ml | 5.0000E+05 | 2.0000E+05 | 3.0000E+05 |
| Cells/L | 5.0000E+08 | 2.0000E+08 | 3.0000E+08 |
| Molecular Weight of 1 EF1 genome | 7.05E+08 | 7.05E+08 | 7.05E+08 |
| MW total (Da or AMU) | 3.5229E+17 | 1.4092E+17 | 2.1138E+17 |
| Expected amount of DNA (ug) | 0.584994577 | 0.233997831 | 0.350996746 |
| Actual Concentrations | | | |
| First Elution (ng) | 1.19 | 0.659 | 0.572 |
| Second Elution (ng) | 1.22 | 0.167 | 0.075 |
| Total (ug) | 0.241 | 0.0413 | 0.03235 |
| Percent Yield | 41.19696308 | 17.64973626 | 9.216609652 |

CURRICULUM VITAE

Vega Shah

vs1@uw.edu (626) 864 6103

Center for Environmental Genomics

Benjamin Hall IRB, 616 NE Northlake Pl, Seattle WA 98105

EDUCATION

- **University of Washington, Seattle**
Ph.D., Biological Oceanography, January 2018
M.S., Biological Oceanography, 2015
- **University of California, Berkeley**
B.S. Environmental Sciences conc. Biology, 2010

RESEARCH EXPERIENCE

- **Pre-Doctoral Research Associate**
University of Washington, September 2011-Present
Description: Physiological, genomic and proteomic analysis of bacteria in low oxygen zones of the ocean.
Duties:
 - **Laboratory:** field sample collection, anaerobic bacterial cultivation, physiology experiments, marine chemical analyses (CHN, DOC and dissolved gases), flow cytometry, electron and epifluorescence microscopy (FISH); DNA, RNA and protein extraction, PCR, qPCR, DNA sequencing, fingerprinting, 16S clone library analysis, 16S phylogeny
 - **Computational:** identification, annotation and statistical analysis of data using R, Python, Geneious and MS Excel; making scientific figures using R, Adobe Illustrator
 - **Supervisory:** Training lab personnel and undergraduate researchers, instructing undergraduate level courses
- **Junior Specialist**
University of California, Berkeley, September 2010-September 2011
Description: Cultivation of novel anaerobic bacteria and study of their activity in extreme habitats like acid mine drainage systems and uranium contaminated ground water
Duties: bacterial culture, electron and epifluorescence microscopy (FISH); DNA, RNA and protein extraction, PCR, qPCR, DNA sequencing, ordering of lab equipment and maintaining inventory
- **Laboratory Technician**
University of California, Berkeley, February 2009-December 2010
Description: Investigating modes of transmission & spread of plant diseases by plant fluid feeding leafhoppers. Examination of insect behavior, plant-arthropod interactions and insect-microbe interactions.
Duties: maintaining bacterial cultivation, upkeep of plants in a greenhouse, DNA extraction, PCR and sequencing, phylogenetic identification of bacteria

PUBLICATIONS

- Shah, V., Zhao, X., Nicastro, D., Ingalls, A., Morris RM. Sulfur uptake and storage in SUP05 extends the influence of the cryptic marine sulfur cycle to the oxygenated ocean (*in prep*)
- Shah, V., Chang, B. X. & Morris, R. M. Cultivation of a chemoautotroph from the SUP05 clade of marine bacteria that produces nitrite and consumes ammonium. ISME J. 11, 1–9 (2016)
- Shah, V. & Morris, R. M. Genome Sequence of ‘Candidatus Thioglobus autotrophicus’ Strain EF1, a Chemoautotroph from the SUP05 Clade of Marine Gammaproteobacteria. ASM Genome Announc. 3, 6–7 (2015)
- Hauser, D. D. W., Tobin, E. D., Feifel, K. M., Shah, V. & Pietri, D. M. Disciplinary reporting affects the interpretation of climate change impacts in global oceans. Glob. Chang. Biol. 22, 25–43 (2015)
- Merkley, E. D. et al. Changes in Protein Expression Across Laboratory and Field Experiment in Geobacter bemidjensis. J. Proteome Res. 150203133548007 (2015)
- Justice, N. B. et al. Heterotrophic archaea contribute to carbon cycling in low-pH, suboxic biofilm communities. Appl. Environ. Microbiol. 78, 8321–8330 (2012).

PRESENTATIONS

- **Ocean Sciences Meeting, 2018**
Chemoautotrophic SUP05 cells boost carbon fixation in oxygenated waters (Poster)
- **Ocean Sciences Meeting, 2016**
Denitrifying SUP05 bacteria require exogenous nitrogen (Poster)
- **Ocean Sciences Meeting, 2014**
Culture and Genomic Potential of SUP05 bacteria (Oral)
- **Integrative Graduate Education and Research Traineeship Conference, 2012**
Dynamics of Ocean Change: How does current science define changing oceans? (Poster)
- **Subsurface Biogeochemical Research Conference, Department of Energy, 2011**
3D Reconstruction of Biological Organization and Mineralization in Sediment Attached Biofilms During Uranium Bio-remediation (Poster)

AWARDS/GRANTS

- **Science Communication Fellowship (Pacific Science Center), 2015**
National Science Foundation funded initiative to train early career scientists in effective public communication
- **NSF Graduate Fellowship (IGERT), 2011-2013**
National Science Foundation’s Integrative Graduate Education and Research Traineeship to train students on the topic of Ocean and Climate Change
- **Schwabacher Grant 2009**
Awarded by College of Natural Resources, University of California, Berkeley
- **NSF REU Grant 2007 and 2008**
Funding for summer undergraduate research experience

TEACHING/SCIENCE COMMUNICATION

- **Meet a Scientist' at Pacific Science Center**
Engaging the public in discussions about science and research
- **Graduate Student Instructor, University of Washington**
OCN 210: Integrative Oceans, Spring 2017
OCN 443: Oceanography Senior Thesis, Fall 2015
OCN 200: Introduction to Oceanography, Fall 2013 and 2015
OCN 102: The Changing Oceans, Winter 2014, 2015 & 2017